

4-28-2006

## Manipulation of Polystyrene Microparticles on a Microchannel Glass

Ravi Mamillapalli  
*Wright State University*

Henry D. Young  
*Wright State University - Main Campus*

Follow this and additional works at: [https://corescholar.libraries.wright.edu/etd\\_all](https://corescholar.libraries.wright.edu/etd_all)



Part of the [Mechanical Engineering Commons](#)

---

### Repository Citation

Mamillapalli, Ravi and Young, Henry D., "Manipulation of Polystyrene Microparticles on a Microchannel Glass" (2006). *Browse all Theses and Dissertations*. 2083.  
[https://corescholar.libraries.wright.edu/etd\\_all/2083](https://corescholar.libraries.wright.edu/etd_all/2083)

This Thesis is brought to you for free and open access by the Theses and Dissertations at CORE Scholar. It has been accepted for inclusion in Browse all Theses and Dissertations by an authorized administrator of CORE Scholar. For more information, please contact [library-corescholar@wright.edu](mailto:library-corescholar@wright.edu).

MANIPULATION OF POLYSTYRENE MICROPARTICLES ON A  
MICROCHANNEL GLASS

April 26, 2006

I HEREBY RECOMMEND THAT THE THESIS PREPARED UNDER MY SUPERVISION  
BY Ravi Mamillapalli TITLED

Manipulation of Polystyrene microparticles on a Microchannel glass

A thesis submitted in partial fulfillment  
of the requirements for the degree of  
Master of Science in Engineering



Henry Daniel Young, Ph.D.  
Thesis Director


By



Richard J. Bertka, Ph.D.  
Department Chair

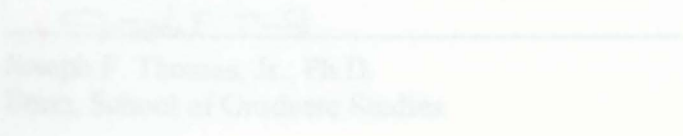
Ravi Mamillapalli

B.E., National Institute of Technology Karnataka  
(formerly KREC Surathkal), India 2002



2005

Wright State University



Joseph P. Thomas, Jr., Ph.D.  
Dean, School of Graduate Studies

WRIGHT STATE UNIVERSITY  
SCHOOL OF GRADUATE STUDIES

April 28, 2006

I HEREBY RECOMMEND THAT THE THESIS PREPARED UNDER MY SUPERVISION  
BY Ravi Mamillapalli ENTITLED  
Manipulation of Polystyrene microparticles on a Microchannel glass  
BE ACCEPTED IN PARTIAL FULFILLMENT OF THE  
REQUIREMENTS FOR THE DEGREE OF  
MASTER OF SCIENCE IN ENGINEERING

\_\_\_\_\_  
Henry Daniel Young, Ph.D.  
Thesis Director

\_\_\_\_\_  
Richard J. Bethke, Ph.D.  
Department Chair

Committee on  
Final Examination

\_\_\_\_\_  
Henry Daniel Young, Ph.D.

\_\_\_\_\_  
Raghavan Srinivasan, Ph.D.

\_\_\_\_\_  
Sharmila M. Mukhopadhyay, Ph.D.

\_\_\_\_\_  
Joseph F. Thomas, Jr., Ph.D.  
Dean, School of Graduate Studies

## ABSTRACT

Mamillapalli, Ravi, M.S.Egr, Department of Mechanical and Materials Engineering, Wright State University, 2006. Manipulation of Microbeads on a Microchannel glass.

Bulk quantities of spherical microbeads have various applications in research and industrial fields. Simple techniques are required to be developed in order to manipulate and modify large numbers of these beads simultaneously. In our experiment, a microchannel glass-based microfluidic device is used to actuate large numbers of microbeads in parallel. The microchannel glass used in these experiments contains channels 4.1  $\mu\text{m}$  in diameter. The microbeads are polystyrene beads which are superparamagnetic in nature and 5-6  $\mu\text{m}$  in diameter. An aqueous suspension of microbeads is injected into a 2-chamber fluid cell that contains a separator, microchannel glass. The beads are reversibly immobilized on the surface of the microchannel glass by the application of suction with the help of a syringe pump. Assessment of bead movement is performed using optical microscopy. Optical micrographs and the live video for various experimental results are presented. Several experiments were performed by varying flow rates in order to manipulate the beads and the data of flow rates is tabulated. The speed of the beads is calculated and is correlated with flow rates in different chambers. The results were studied by plotting the flow rates and speed of the beads. Microbeads are also immobilized by applying pressure in fluid cell. The pressure is applied by weights suspended and held on syringes at respective positions. Several experiments are performed by applying varied pressures in different chambers and these pressures are plotted. Optical micrographs and the live video for various applied pressures are presented.

# Contents

<b>1 Introduction</b> .....	<b>1</b>
1.1 Overview.....	1
1.2 Applications of microbeads.....	4
1.3 Techniques of manipulation of microbeads.....	7
1.3.1 Optical tweezers.....	7
1.3.2 Laser tweezers.....	8
1.3.2.a Trajectory control of multiple objects by laser manipulation.....	9
1.3.3 Magnetic tweezers.....	10
1.3.4 Dielectrophoresis.....	12
1.3.5 Atomic force microscopy.....	13
1.3.6 3D Magnetic force microscope (3DMFM).....	14
1.3.7 Acoustic particle manipulation.....	16
1.4 Limitations.....	18
1.5 Thesis organization.....	19
<b>2 Fundamentals and Related work</b> .....	<b>20</b>
2.1 Fundamentals of manipulation of microbeads on microchannel glass.....	20
2.2 Literature review.....	22
2.2.1 Microbeads background.....	22
2.2.2 Microchannel glass.....	26
2.2.3 Microchannel plate technology.....	29
<b>3 Experimental setup</b> .....	<b>30</b>
3.1 Introduction.....	30
3.2 Microchannel glass sample preparation.....	32
3.2.1 Sample mounting.....	32
3.2.2 Polishing.....	32
3.2.2a Polishing methods.....	33
3.2.3 Etching.....	33
3.3 Equipment used.....	38
3.3.1 Hot plate.....	38
3.3.2 Stirring plate.....	38
3.3.3 Dual syringe pump.....	38
3.3.3a Loading syringes.....	39
3.3.4 Optical microscopy.....	40
3.3.5 To find the allowable and desirable flow rates.....	41
3.4 Challenges in making fluid cell.....	44
<b>4 Experiments</b> .....	<b>47</b>
4.1 Experimental procedure.....	47
4.2 Precautionary measures.....	48
4.3 Manipulation of beads by applying flow rate.....	49
4.4 Manipulation of beads by applying pressure.....	53
<b>5 Results and Discussion</b> .....	<b>53</b>
<b>6 Conclusions and future work</b> .....	<b>82</b>
<b>REFERENCES</b> .....	<b>83</b>

## LIST OF FIGURES

Figure 1.1 8 a) Optical trap hold particle at center b) Interaction of particle with light ....	8
Figure 1.2 Schematic diagram of Laser activated manipulating experimental system.....	10
Figure 1.3 Schematic diagram of magnetic manipulation.....	11
Figure 1.4 Moving neutral particles: dielectrophoresis.....	12
Figure 1.5 Atomic force microscope with force applied on bead by tip.....	14
Figure 1.6 Input and Output signals for the 3D force microscope.....	15
Figure 1.7 Pull of particle to transverse velocity antinodes.....	16
Figure 1.8 Separation of microbeads and air bubbles inside the capillary.....	17
Figure 2.1 Fabrication process of Microchannel glass.....	27
Figure 3.1 Top view and front view of Fluid cell model.....	31
Figure 3.2 Etching setup for microchannel glass.....	35
Figure 3.2 SEM micrograph of microchannel glass at 7800X magnification and 25 kV..	36
Figure 3.4 SEM micrograph of microbeads at 3000X magnification and 8 kV.....	37
Figure 3.5 Spectrum of Microbeads from EDS.....	37
Figure 3.6 loading of syringes on syringe pump.....	39
Figure 3.7 The Fluid cell setup with Different flow rates and velocities at outlets.....	41
Figure 3.8 Microchannel glass with average field count 1025.....	42
Figure 3.6 Solid works design of the fluid cell model.....	45
Figure 4.1 Experimental setup of fluid cell and syringe pump.....	49
Figure 4.2 Fluid Cell Experiment Setup with pressure applied.....	51
Figure 5.1 Flow rate in upper chamber $F_a$ vs Flow rate in lower chamber $F_c$ & $F_a$ vs critical $F_c$ .....	56
Figure 5.2 Velocity of flow $V$ vs Flow rate in upper chamber $F_a$ .....	56
Figure 5.3 Flow through bent tube from A to B and pressure loss in tube.....	60
Figure 5.4 Moody chart with Reynolds number vs Friction factor.....	63
Figure 5.5 $P_a$ vs $P_c$ values.....	66
Figure 5.6 Microbeads arraying on Microchannel glass.....	68
Figure 5.7 Microbeads arraying on Microchannel glass.....	69
Figure 5.8 Microbeads arraying on Microchannel glass.....	70
Figure 5.9 Microbeads arraying on Microchannel glass.....	70
Figure 5.10 Microbeads arraying on Microchannel glass.....	71
Figure 5.11 Microbeads arraying on Microchannel glass.....	72
Figure 5.12 Microbeads arraying on Microchannel glass.....	72
Figure 5.13 Microbeads arraying on Microchannel glass.....	73
Figure 5.14 Clumping of microbeads on microchannel glass.....	73
Figure 5.15 Microbeads arraying on Microchannel glass.....	74
Figure 5.16 Microbeads arraying on Microchannel glass.....	75
Figure 5.17 Clumping of microbeads on microchannel glass.....	75
Figure 5.18 Microbeads struck in channels of microchannel glass.....	77
Figure 5.19 Microbeads struck in channels of microchannel glass.....	78
Figure 5.20 Microbeads struck in channels of microchannel glass.....	79
Figure 5.21 Microbeads struck in channels of microchannel glass.....	80
Figure 5.22 Microbeads struck in channels of microchannel glass.....	81
Figure 5.23 Microbeads struck in channels of microchannel glass.....	82

**LIST OF TABLES**

Table 3.1 The Inlet flow rate as against velocity of beads flow.....43  
Table 3.2. Tabulation of Flow rate through channels of microchannel glass as against velocity of beads through channels.....43  
Table 5.1 Velocity of flow values corresponding to  $F_a$  and  $F_c$  values.....54  
Table 5.2 Critical  $F_c$  values vs  $F_a$  values.....55  
Table 5.3 Velocity of bead flow in upper chamber to corresponding weights at A ( $m_a$ ) and C ( $m_c$ ).....58  
Table 5.4  $m_a/m_b$  values after friction loss weight in grams..... 58  
Table 5.5  $m_c$  values after friction loss weight in grams.....59  
Table 5.6 Flow rate in tube  $Q_T$  vs Velocity of flow of beads in tube  $V_T$ .....62  
Table 5.7 Reynolds number, friction factor, (m/s)  $V_T$  values of flow in the tube.....64  
Table 5.8  $P'a$ ,  $P'c$  values with critical arraying  $P'c^*$  and critical clumping  $P'c^{\wedge}$  values to corresponding  $P'a$  values .....66

# 1 Introduction

## 1.1 Overview

### ACKNOWLEDGEMENTS

I express my sincere gratitude and appreciation to my thesis advisor Dr. Daniel Young for his guidance, suggestions, and comments throughout the course of my work. His support has been invaluable and a constant encouragement in the accomplishment of my thesis. This work would not have been completed without his help. I would like to thank Dr. Ron Tonucci for his immense help providing me micro channel glass specimen for my thesis and lending advice during my thesis work. I am grateful to him for his constant guidance throughout my thesis work. I would also like to thank Dr. Raghavan Srinivasan and Dr Sharmila M Mukhopadhyay for being a part of my thesis committee and giving me helpful comments and suggestions. The suggestions and guidance of Dr. Mostafa El-Ashry were of immense help and are highly appreciated. I want to extend my acknowledgements to Dr. Richard Bethke, and all the staff of Mechanical Engineering for providing me the entire necessary infrastructure for the successful completion of my thesis.

Finally, I would like to dedicate this work to my loving parents and my dearest brothers. Their love, support, and encouragement made it easier for me to reach my academic goal. I would like to thank all my friends and my roommates for providing me the strength and support during my stay in the US.



# 1 Introduction

## 1.1 Overview

Microparticle technology is one of the emerging technologies in materials science and biomedical fields. Microparticles can be different by their diameters, polymer chemistries, densities, refractive indices, surface charges and surface functional groups. In general, microparticles are at micron range and have excellent physical and chemical properties such as uniform spherical size, monodispersity, mechanical stability. Polystyrene microbeads are one of the types of microparticles which have several clinical and biomedical applications. The microbeads vary depending on their morphology and composition. The microbeads are mostly polymeric and ceramic in nature. They are made as per different applications. The manipulation of these polystyrene microbeads is very important because of these varied applications. Manipulation of microparticles is very difficult because of working at a size of micron-level. Moreover it is easy to handle one microbead or microparticle at a time. However to handle a bulk number of beads at a time is challenging. The manipulation of microbeads in general, can be done in different ways. They are magnetic manipulation, laser tweezers, acoustic manipulation, optical tweezers, dielectrophoresis and atomic force microscopic manipulations. The manipulation techniques are elaborated in coming sections. The techniques provide a means by which individual molecules can be sorted and manipulated in order to alter the physical or chemical reaction pathways that occur in biological organisms at the most fundamental level.<sup>1</sup>The different types of manipulation of microbeads differ depending on the type of application it requires and for example for drug targeting, magnetic manipulation of beads is required. For an optical spin micrometer to run, optical tweezers is required, where radiant energy is converted to mechanical energy.<sup>2</sup> The microbeads are to be half-coated for specific applications such as microfabrication and micromachining. Hence for the beads to

half-coated, they have to be manipulated and placed in such a way that half the area is exposed. For that they can be manipulated by applying suction and made to occupy the channels on microchannel glass. The beads cannot be manipulated by other techniques in such a way that half of the beads are exposed and handled on a specimen. Hence the technique of manipulation of microbeads on microchannel glass is useful, when compared to other techniques of manipulation and our technique is employed for this specific application of partial coating of bead, micromachining and microfabrication. Moreover the beads are to be placed in an array to make all the beads half-coated simultaneously.

In this thesis, the manipulation of polystyrene microbeads is performed on a microchannel glass. Microchannel glass is made of glass with uniform and parallel channels of diameter about  $\sim 200\text{nm}$  to  $\sim 5\mu\text{m}$ . The fabrication of microchannel glass is obtained by a draw process, where there is an insertion of a cylindrical acid-etchable glass rod (channel glass) into an inert glass tube (matrix glass). The pair is then drawn at high temperature under vacuum to reduce the over all cross section to that of a fine filament. The filaments are then stacked in a bundle, refused and redrawn until appropriate channel diameters and desired number of array elements are achieved. The microchannel glass has a composite glass structure with aspect ratio and it is thermally stable. The microchannel glass can be etched by acids.

The microchannel glass used in this thesis is of  $4\text{-}5\mu\text{m}$  diameter. The microchannel glass is polished, chemically etched and then placed in a two-chamber fluid cell where the polystyrene microbeads solution is injected with the help of syringes. The microbeads are manipulated on the microchannel glass, in fluid cell, by changing flow rates with the help of syringe pump. The microbeads can also be manipulated on the microchannel glass by applying pressure on the beads in the fluid cell. The pressure can be created by applying weights on the syringes. The flow rates in both chambers are measured and are plotted. These plots are studied

and the corresponding optical micrographs are taken for several flow rates and pressures applied. The video of the microbeads flow is also recorded when flow rates and pressure are applied. The manipulation of beads on a microchannel glass has applications such as microfabrication and micromachining.

Magnetic particle hyperthermia is appealing because it offers a way to ensure that only the intended target tissue is heated. The concept is based on the principle that a magnetic microbead can generate heat by hysteresis loss when placed in a high-frequency (~1 MHz) magnetic field. The principle of heating with superparamagnetic particles (that show no magnetic hysteresis at low frequencies) by an AC field has been reviewed.<sup>2</sup>

Magnetic beads can also play a vital role in drug targeting, as they can be vectors for carrying the drug and can be magnetically guided to the desired location. In magnetically targeted therapy, a cytotoxic drug is attached to biocompatible magnetic carriers that are injected into the patient via the circulatory system. Larger particles with dimension > 10 μm, comprising agglomerates of superparamagnetic particles, were shown to be more effective in withstanding flow dynamics within the circulatory system.<sup>3</sup>

Biosensors are constructed for monitoring a biological reaction at surface of electrodes. A variety of biomolecules have been used as basic detection elements of AC biosensors with different degrees of success. Enzymes, antibodies, nucleic acids, cells and microorganisms have been immobilized onto the surface of electrodes by microbeads to develop biosensors.<sup>4</sup>

The polystyrene microbeads have applications in Microchips areas such as lab-on-chip. In operation, a micropump sends 1-microliter samples of 10-micrometer-diameter surface-coated beads (for detecting surface agents) or human cells (for detecting disease) into the

## 1.2 Applications of Microbeads

Microbeads have applications such as drug targeting, hyperthermia, optical encoding in BioMEMS, Lab-on-chips, collecting bacteria from milk and food and assay systems. Hyperthermia is one of the most promising approaches in cancer therapy: it consists in heating and destroying the target tissue. The problem with hyperthermia is the difficulty of local heating of only the tumor region until the required temperature is reached, without damaging the surrounding normal tissue. Magnetic particle hyperthermia is appealing because it offers a way to ensure that only the intended target tissue is heated. The concept is based on the principle that a magnetic microbead can generate heat by hysteresis loss when placed in a high-frequency ( $\sim 1$  MHz) magnetic field. The principle of heating with superparamagnetic particles (that show no magnetic hysteresis at low frequencies) by an AC field has been reviewed.<sup>3</sup>

Magnetic beads can also play a vital role in drug targeting, as they can be vectors for carrying the drug and can be magnetically guided to the desired location. In magnetically targeted therapy, a cytotoxic drug is attached to biocompatible magnetic carriers that are injected into the patient via the circulatory system. Larger particles with dimension  $> \mu\text{m}$ , comprising agglomerates of superparamagnetic particles, were shown to be more effective in withstanding flow dynamics within the circulatory system.<sup>3</sup>

Biosensors are constructed for monitoring a biological reaction at surface of electrodes. A variety of biomolecules have been used as basic detection elements of AC biosensors with different degrees of success. Enzymes, antibodies, nucleic acids, cells and microorganisms have been immobilized onto the surface of electrodes by microbeads to develop biosensors.<sup>4</sup>

The polystyrene microbeads have applications in Microchips areas such as lab-on-chip. In operation, a micropump sends 1-microliter samples of 10-micrometer-diameter surface-coated beads (for detecting warfare agents) or human cells (for detecting disease) into the

microchannel of chip. Manipulation of beads in a microchip is not always trivial but could be well packed for the detection and characterization of affinity reactions within the microchannel and combined the use of microbeads in a microfluidic system with integrated microelectrode arrays for detection of small molecules.<sup>5</sup> The manipulation and trapping of microbeads in a channel of microchip using fluid flow only. The capture and preconcentration of beads and molecular species is possible in these flows.<sup>6</sup>

The development of optically encoded microbeads for massively parallel and high throughput analysis of biological molecules is reviewed. The encoded bead technology is based on the optical properties of semiconductor QDs(quantum dots) and these have to be incorporated into the beads at controlled ratios. The cross-linked polystyrene microbeads are well suited for QDs incorporation.<sup>7</sup>

Large, antibody fragment-coated polystyrene beads have been used to collect bacteria from milk, water and food.<sup>8</sup> Silica microspheres are naturally hydrophilic. Hence no protein should adsorb nonspecifically onto these silica microspheres. After covalent attachment, only the desired antigen-antibody reaction should occur. The difference in density between silica and polystyrene (1.96 g/ml for silica versus 1.05 for polystyrene) dictates a critical difference in settling velocity. Because settling in water depends on the difference in density between microspheres and water ( $1.96 - 1.00 = 0.96$  for silica;  $1.05 - 1.00 = 0.05$  for polystyrene), the silica microspheres will settle about 19 times as fast as the polystyrene. This difference in settling velocity could be exploited in some interesting tests and assays based on differential settling times of agglutinated and unagglutinated microspheres. Hence during assaying the silica microspheres are not as good as polystyrene beads as their settling velocity is more.<sup>8</sup>

Superparamagnetic particles have been utilized extensively in diagnostics and other research applications for the capture of biomolecules and cells. They confer a number of

benefits, including ease of separation and suitability for automation. Highly efficient magnetic separations have also led to improvements in applications such as separations of cells from polystyrene magnetic beads.<sup>2</sup>

The understanding of photonic crystals based on colloidal crystal growth is an important approach to microfabrication. Colloidal crystallization occurs through highly monodispersed, micrometer-sized polymer or silica spheres in arrays.<sup>10</sup> In optical spin micrometer, a large bead is trapped by optical tweezers, which rotates around the laser beam axis. The small bead is coated with gold for generating the spin torque through the change of momentum from gradient radiation pressure of the laser applied on coated small bead.<sup>2</sup>

A dot-array of self-assembled and self-sorted polymer beads for analytical and biochemical screening has been generated and beads are immobilized in a printed pattern.<sup>11</sup>

The half coating of bead can be done if they are manipulated on microchannel glass as half of the beads are trapped in the channels of microchannel glass during manipulation.

### 1.3.1 Optical tweezers

This means if its direction is changed by an object then that object will feel a force exerted on it. We can use this to move a tiny particle which is called optical tweezing. Dielectric beads are attached to either end of a piece of DNA and Optical tweezers can be used to look at the mechanical properties of the DNA molecule. So this leads to better understanding of structure and function of DNA. The radiation pressure exerted by optical tweezers is used for investigating mechanical structure of cells (red blood cells).<sup>12</sup>

The most basic form of an optical trap is shown in Figure 1.1a. A laser beam is focused to a spot by a high-quality microscope objective in the specimen plane. This spot creates an "optical trap" which can hold a small particle at its center. The forces felt by this particle are light scattering and gradient forces due to the interaction of the particle with the light (Figure 1.1b). Optical tweezers are built by modifying a standard optical microscope. These

## 1.3 Techniques for Manipulation of Microbeads

Manipulation of microparticles is very difficult as discussed. There are different techniques of manipulating the microbeads. These techniques are developed keeping in mind the applications of the microbeads. The motivation behind developing single molecule measurement techniques is to probe information about the statistical distributions of biological systems that would be otherwise obscured by ensemble measurements. These techniques also provide a means by which individual molecule can be sorted and manipulated in order to alter the physical or chemical reaction pathways that occur in biological organisms at the most fundamental level. The different techniques for manipulation of microparticles are optical tweezers, laser tweezers, magnetic tweezers, electrophoretic translocation or dielectrophoresis, and acoustic particle manipulation, atomic force microscopy, micropipettes.

### 1.3.1 Optical tweezers

Light can behave like particles (called photons) and hence has momentum. This means if its direction is changed by an object then that object will feel a force exerted on it. We can use this to move a tiny particle which is called optical tweezing. Dielectric beads are attached to either end of a piece of DNA and Optical tweezers can be used to look at the mechanical properties of the DNA molecule. So this leads to better understanding of structure and function of DNA. The radiation pressure exerted by optical tweezers is used for investigating mechanical structure of cells (red blood cells).<sup>12</sup>

The most basic form of an optical trap is shown in Figure 1.1a. A laser beam is focused to a spot by a high-quality microscope objective in the specimen plane. This spot creates an "optical trap" which can hold a small particle at its center. The forces felt by this particle are light scattering and gradient forces due to the interaction of the particle with the light (Figure 1.1b). Optical tweezers are built by modifying a standard optical microscope. These

instruments can manipulate micron-sized objects to sophisticated devices with the aid of computer-controls which can measure displacements and forces with high precision and accuracy.<sup>12</sup>

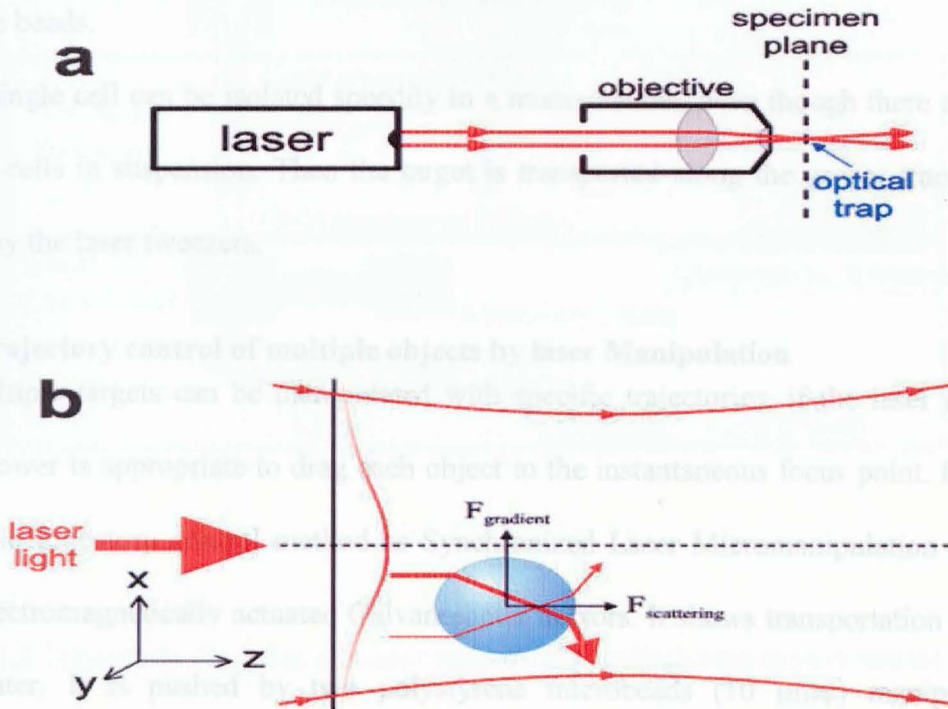


Figure 1.1 a) Optical trap hold particle at center b) Interaction of particle with light<sup>12</sup>

Optical tweezers involve tethering biological molecules to dielectric spheres and then capturing the spheres at focal point of an electric field gradient. These tweezers can selectively manipulate a single molecule and manipulate each end of a molecule independently.<sup>12</sup> The array of tweezing spots is selectively filled with microbeads and trap more beads with maximum laser power. The beads are also formed as an array of mosaic or alphabetical order by the optical trapping.<sup>13</sup>

### 1.3.2 Laser tweezers

Laser tweezers have been used for manipulation of particles in closed spaces. They are utilized for manipulation of biological objects such as viruses and bacteria. The direct



irradiation of focused laser may damage the trapped object. It depends on the target, wave length, irradiation time and power of the laser. Therefore indirect manipulation of the target by the laser trapped microtools is implemented.<sup>14</sup> The cells are manipulated by this method using polystyrene beads.

A single cell can be isolated speedily in a microchannel, even though there are a large number of cells in suspension. Then the target is transported along the proper transportation trajectory by the laser tweezers.

### 1.3.2. a Trajectory control of multiple objects by laser Manipulation

Multiple targets can be manipulated with specific trajectories, if the laser irradiation time and power is appropriate to drag each object to the instantaneous focus point. It refers to this multiple trajectory control method as Synchronized Laser Micromanipulation (SLM). It uses the electromagnetically actuated Galvanometer mirrors. It shows transportation of a yeast cell in water. It is pushed by two polystyrene microbeads (10  $\mu\text{m}\phi$ ) manipulated by Synchronized Laser Micromanipulation.<sup>14</sup>

Alternatively, magnetic tweezers trap magnetic microparticles in tailored magnetic field gradients. Due to the magnetic anisotropy inherent in the particles, rotation of the magnetic poles generating the magnetic field gradients that capture the particles imparts torque to the microparticle and, consequently, to a biological molecule attached to the particle. This torsional motion can be used to stretch, twist, or uncoil the biological molecule with a smaller force than that resulting from lateral displacement of the particle. With this type of tweezers, one end of the biological molecule must be attached to a fixed point, typically a microscope slide.<sup>4</sup>

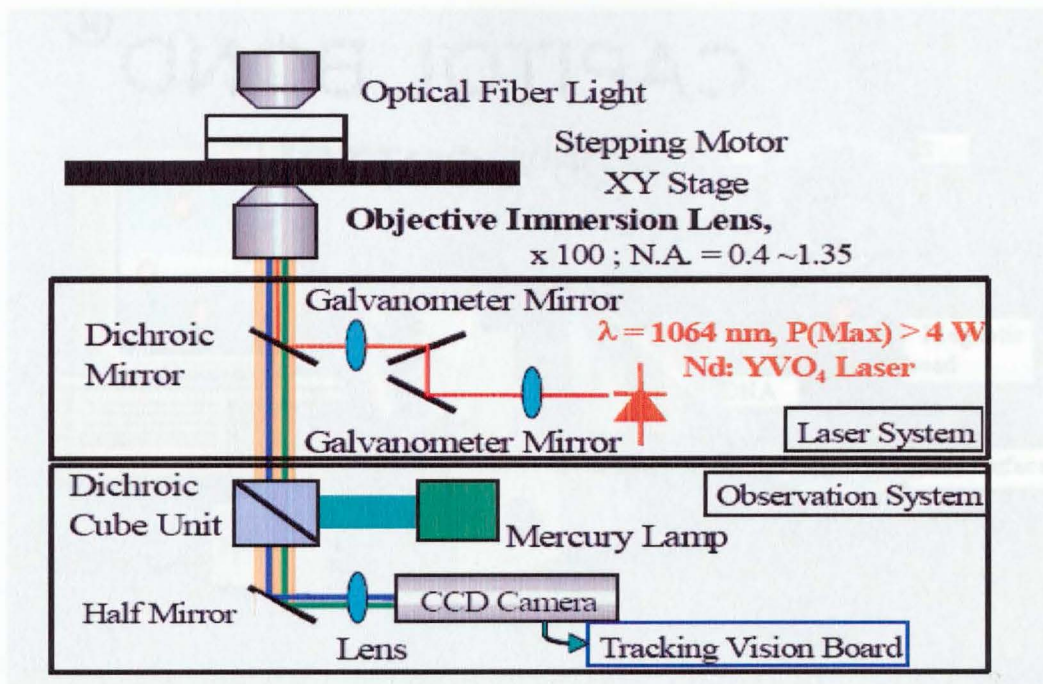


Figure 1.2 Schematic diagram of Laser activated manipulating experimental system <sup>14</sup>

Magnetic micromanipulation of micrometer-sized magnetic particles provides a means

Figure 1.2 Schematic diagram of Laser activated manipulating experimental system <sup>14</sup>

### 1.3.3 Magnetic Tweezers

Alternatively, magnetic tweezers trap magnetic microparticles in tailored magnetic field gradients. Due to the magnetic anisotropy inherent in the particles, rotation of the magnetic poles generating the magnetic field gradients that capture the particles imparts torque to the microparticle and, consequently, to a biological molecule attached to the particle. This torsional motion can be used to stretch, twist, or uncoil the biological molecule with a smaller force than that resulting from lateral displacement of the particle. With this type of tweezers, higher forces can be attained. Because of their low power requirements, miniature systems can be applied to multiple magnetic particles over large distances and also track magnetically labeled molecules and cells for applications, such as cell-based biosensors and gene expression monitoring, as well as directed cell assembly for tissue engineering. <sup>1</sup>

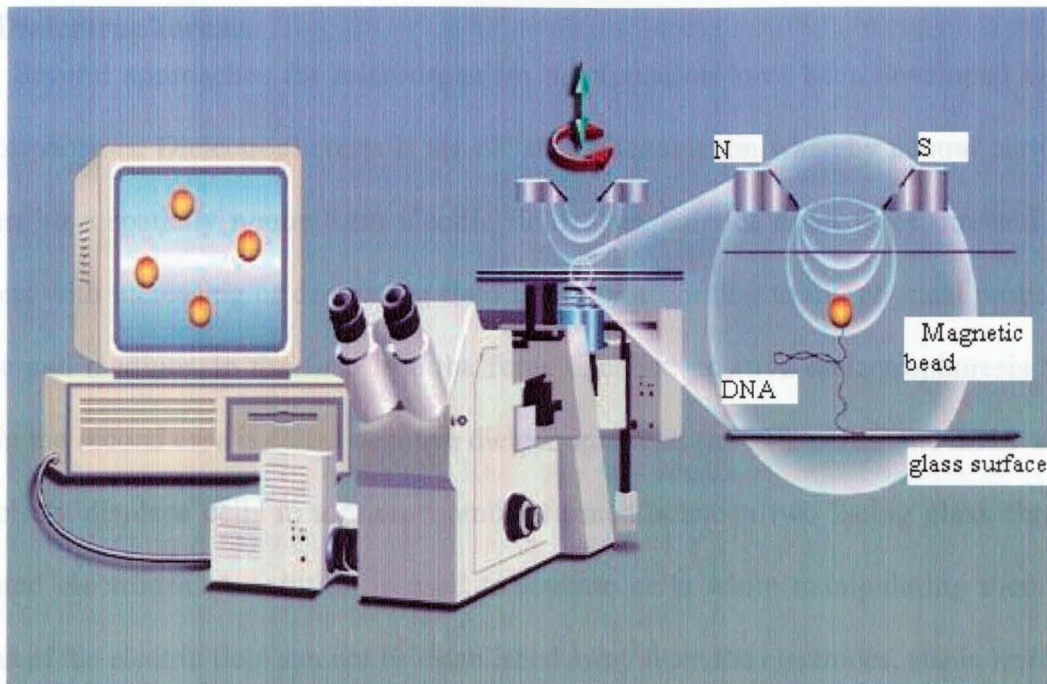


**Figure1.3 Schematic diagram of Magnetic manipulation** <sup>15</sup>

Magnetic micromanipulation of micrometer-sized magnetic particles provides a means to probe molecular binding interactions, separate biological materials, characterize cell mechanical properties and control biochemical activities and gene expression within living cells. Existing magnetic manipulation techniques apply controlled mechanical stress to magnetic particles by generating either large magnetic field gradients to apply directed forces or alternating magnetic field orientations to apply torques. Magnetic methods provide advantages over other techniques like optical tweezers, for large scale separation of materials, manipulation of microparticles, and mechanical analysis of living cells because magnetic gradients can be applied to multiple magnetic particles over large distances and also much higher forces can be attained. Because of their low power requirements, miniature electromagnets may also be useful to non-invasively control the position and function of magnetically labeled molecules and cells for applications, such as cell-based biosensors and bioprocessors, as well as directed cell assembly for tissue engineering.<sup>16</sup>

### 1.3.4 Dielectrophoresis

Several approaches for microorganism manipulation have been developed based on dielectrophoresis. Dielectrophoresis is the physical phenomenon whereby neutral particles, in response to a spatially nonuniform electric field  $E$ , experience a net force directed toward locations with increasing or decreasing field intensity according to the physical properties of particle and medium. In the first case the force is called positive dielectrophoresis (pDEP) while in the second case is called negative dielectrophoresis (nDEP). pDEP and nDEP are used to precisely displace cells in a microchamber formed between two facing glass chips with elongated electrodes. A solution is used to levitate cells while manipulating them. Since maxima of the electric field can not be established away from the electrodes, stable levitation is possible only with nDEP force. <sup>17</sup>

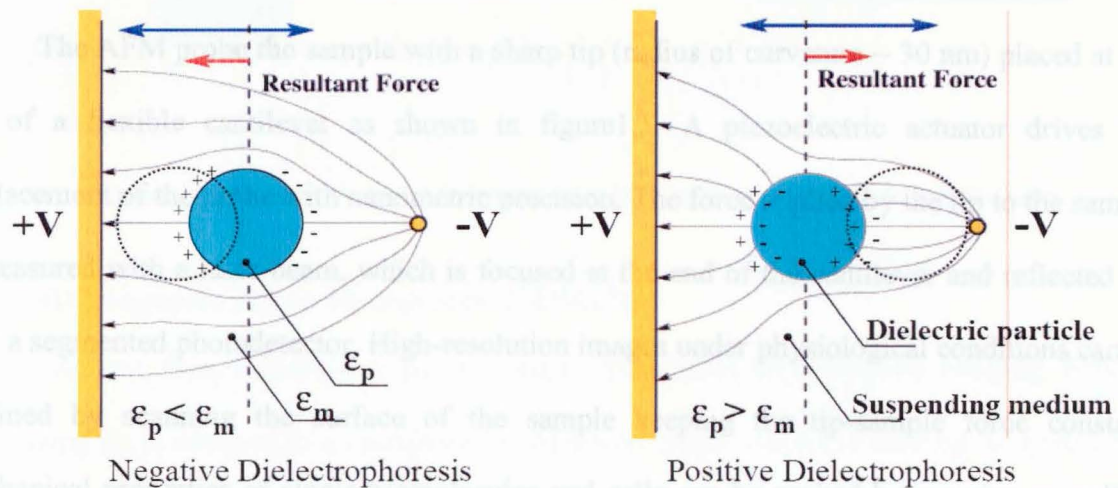


Figure 1.4 Moving neutral particles: Dielectrophoresis <sup>18</sup>

Separation of microbeads can be done by nDEP. The dielectrophoretic force depends on particle size and on magnitude of non-uniformity of applied electric field. The polarity of

this force depends on the polarity of the induced dipole moment, which in turn is determined by the conductivity and permittivities of the particle and its suspending medium. The yeast cells and microbeads are trapped in nDEP cages and yeast cells are attracted toward electrode borders. So microbeads move from cage and yeast cells are newly trapped. With this we can manipulate some tumor cells and separate white and red blood cells.

### 1.3.5 Atomic force microscopy

The mechanical properties of the cell play an important role in essential cellular functions including mechanotransduction, shape stability, adhesion, motility and gene expression. Nanotechnology enables manipulation of matter with nanometric and picoNewton precision, providing innovative approaches for studying the structure and function of single biomolecules and cells under physiological conditions.<sup>19</sup>

The AFM probe the sample with a sharp tip (radius of curvature  $\sim 30$  nm) placed at the end of a flexible cantilever as shown in figure1.5. A piezoelectric actuator drives 3D displacement of the probe with nanometric precision. The force applied by the tip to the sample is measured with a laser beam, which is focused at the end of the cantilever and reflected off onto a segmented photodetector. High-resolution images under physiological conditions can be obtained by scanning the surface of the sample keeping the tip-sample force constant. Mechanical properties of single biomolecules and cells can be probed by pressing or pulling the sample with the tip and measuring the force-displacement relationship. Ligand-receptor adhesion can be probed by coating tip with ligands to cell membrane receptors.<sup>19</sup>

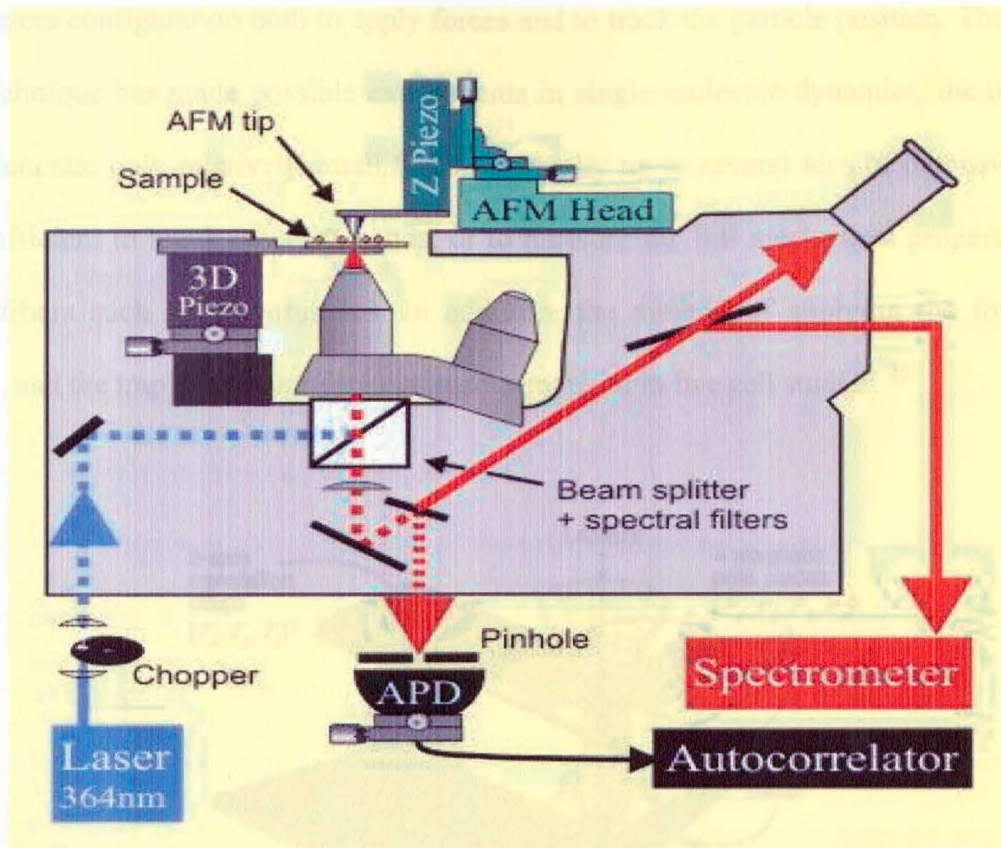


Figure 1.5 Atomic Force Microscope with force applied on bead by tip<sup>19</sup>

### 1.3.6 3D Magnetic Force Microscope (3DMFM)

Atomic force microscopy has two major drawbacks for biological imaging. First, the measuring tip is attached to a cantilever for position control and force sensing. It cannot probe beneath objects; we can image only the tops of surface-bound objects. Second, present-day microscopes cannot go inside living cells, because the cantilever would have to protrude through the cell membrane.<sup>20</sup>

If the tip is allowed to free it from the cantilever, then the problems are alleviated. It has needs to implement new ways of force generation and position sensing. The current implementation of a 3D force microscope (3DFM) using a free particle uses an optical beam in

a laser tweezers configuration both to apply forces and to track the particle position. The laser tweezers technique has made possible experiments in single molecule dynamics, the optical beam can generate only relatively small forces, normally up to several tens of piconewtons. This is insufficient to break covalent bonds, or to measure the full mechanical properties of biological fibers such as microtubules. In addition, the method of applying the force is nonspecific, and the trap can accumulate extraneous material in live cell studies. <sup>20</sup>

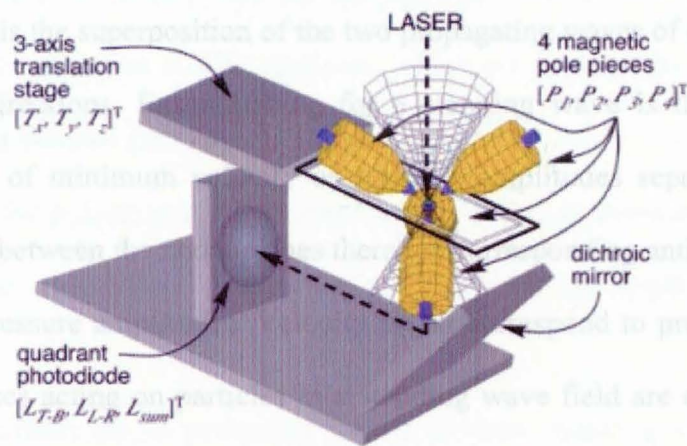


**Figure 1.6 Input and Output signals for the 3D force microscope** <sup>20</sup>

The magnetic beads are used to apply forces in one dimension to cell membranes and to measure the viscosity inside living cell. The optical force microscope (OFM) monitors its particle position with optical light scattering, achieving a resolution on the order of 1nm in all three dimensions. The optical tweezers technique has been demonstrated as a 2D force microscope in the imaging of a surface. The design extends magnetic force control to a 3-D working volume and uses optical light scattering for tracking. It also includes an optical microscope system sharing the same optical path with the laser system, enabling the display of fluorescence and bright field imaging superimposed with the tracked beam information. This

approach has substantial advantages. The force is applied selectively to the magnetic bead, and so it does not directly affect cells or proteins. While exerting forces, the magnetic field does not heat the medium, whereas heating limits the force that can be applied by an OFM.<sup>20</sup>

Figure 1.6 Separation of microbeads and air bubbles towards the capillary, particles are

### 1.3.7 Acoustic particle manipulation

The particles when subjected to an acoustic standing wave were collected in orthogonal lines separated by one half wavelength of sound in the medium. Acoustic particle manipulation has not yet been widely applied and implemented.

A standing wave is the superposition of the two propagating waves of equal amplitude, traveling in opposite directions. Extinguishing for a standing wave is the formation of stationary nodal planes of minimum velocity or pressure amplitudes separated by half a wavelength. Equidistant between the nodal planes there are corresponding anti-nodal planes of maximum velocity or pressure amplitudes. Velocity nodes correspond to pressure antinodes and vice versa. The forces acting on particles in a standing wave field are called acoustical radiation forces and can be separated into the primary radiation forces in axial and transverse direction of sound propagation, and the secondary particle-particle interaction forces originating from scattering of the incident wave.<sup>21</sup>

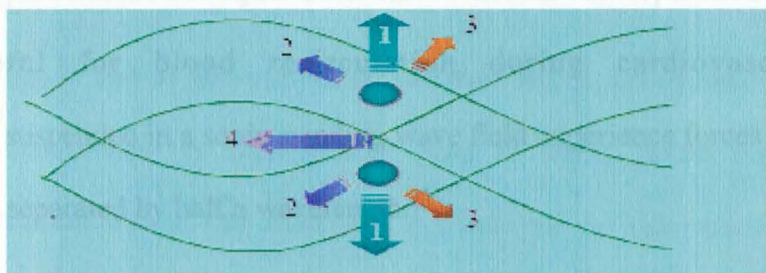
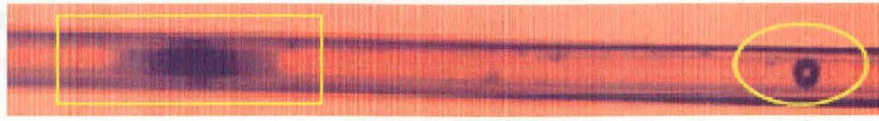


Figure 1.7 pull of particle to transverse velocity antinodes<sup>22</sup>





**Figure 1.8 Separation of microbeads and air bubbles inside the capillary, particles are collected at the transverse velocity antinodes while air bubbles are collected at nodes** <sup>22</sup>

In figure 1.7 particles vibrate in directions 2 and 3. The displacement in vertical direction is less due to space constraint in capillary and particle has little resistance to move in direction 2. Hence net motion is in direction 4. The particles, which are heavier than water move to transverse velocity antinodes and particles which are lighter than water move to velocity nodes as shown in figure 1.8. So the polystyrene microbeads are collected at pressure nodes and the bubbles are collected at antinodes. Thus the microbeads are manipulated by acoustic manipulation. <sup>22</sup>

The main applications are in streaming fluidic devices, standing waves across the passing fluid have been used to separate particles or cells from the fluid flow by using flow splitters. This separation technique can be used to clarify suspensions or to increase the concentration of particles in a sample. So it can be shown that separation of far from blood which is useful for blood recirculation during cardiovascular surgery. <sup>22</sup> Cells or particles suspended in a sonic standing wave field experience forces which concentrate them at positions separated by half a wavelength. <sup>23</sup>

## 1.4 Limitations

The manipulation techniques used for manipulating microbeads discussed above have some limitations. In magnetic tweezers (magnetic force microscopy) the power consumption is more and moreover the particles cannot be sorted into an array for longer periods of time without causing local heating. This may also damage the sample.<sup>24</sup> Limitations have existed as to the applications of optical tweezers, as the number of particles that can be trapped sharing is determined by the refresh time of the individual traps.<sup>25</sup> The Laser tweezing is expensive technique as the lasers cost itself is very high and damage can be caused to particles by laser during irradiation. In dielectrophoresis the variation in geometric parameters were designed to determine the limitations of the process during patterning. The disadvantage in dielectrophoresis is that the particles are localized at the electrodes after separation, and flushing needs to be performed to collect the separated particles.<sup>26</sup> The manipulation of beads by atomic force microscope has a limitation, where the tip can deform the bead if more force is applied on the bead. The microbeads are to be half-coated for specific applications such as microfabrication and micromachining. Hence for the beads to be half-coated, they have to be manipulated and placed in such a way that half the area is only exposed. The beads cannot be manipulated by these techniques in such a way that half of the beads are exposed and handled on a specimen. This is one of the limitations of other techniques. Hence the technique of manipulation of microbeads on microchannel glass is useful, when compared to other techniques of manipulation and our technique is employed for this specific application of partial coating of bead.

## 1.5 Thesis organization

The rest of the chapters of the thesis are organized as follows. Fundamentals of manipulation of microbeads on a microchannel glass and literature review (relevant work) of the field are discussed in Chapter 2. Experimental setup, equipment used in the experiments and for preparation of microchannel glass, optical microscopy, microchannel glass sample preparation and the challenges in making a fluid cell are covered in Chapter 3. The experimental procedure, experiments performed for manipulation of beads in different modes is discussed in Chapter 4. Results and discussions are summarized in Chapter 5. Conclusions, future work and references are listed at the end of the draft.

## **2 Fundamentals and Related Work**

### **2.1 Fundamentals of Manipulation of Microbeads on Microchannel glass**

Manipulation of polystyrene microbeads on a microchannel glass is performed in a fluid cell by applying pressure or through flow rate. This is one of the economical techniques for manipulation of microbeads. The phenomenon behind trapping of microbeads on a microchannel glass is the pressure created by weights suspended and held on the syringes, through which the bead solution is injected. The beads are reversibly immobilized by creating suction in lower chamber and equal pressure at both ends of upper chamber is maintained. So the variation in pressure causes the beads to make a trajectory of motion. The polystyrene beads flow when there is no suction from lower chamber. However as the suction is increased the beads begin to make array on the microchannel glass. The ordering takes place until some critical pressure. After that the beads tend to clump due to high suction in lower chamber. The microbeads are also struck in channels due to variation in size of beads. Hence the size distribution of beads is necessary when we consider the beads struck in channels. All the beads should be of uniform size and diameter more than that of channels, so that the manipulation could give more percentage of arraying of beads.

The microbeads are also manipulated on microchannel glass by applying variable flow rate on the syringes with the help of a syringe pump. The syringes held on syringe pump are connected to fluid cell through tubes. The syringes in upper chamber are made to inject and suck the beads from both sides and vice versa. The lower chamber is connected to another syringe held on other syringe pump through a tube and suction is created in the chamber. The flow rates are automated by syringe pump and they are programmed in such a way that there is a continuous run of beads solution in the upper chamber and the suction is applied in gradual

attrition. As the suction in lower chamber is increased and keeping one of the flow rate in upper chamber at a fixed value. So the injected flow rate in upper chamber is equal to the suction flow rate in upper and lower chambers. There will be flow when there is no suction. However as suction increases the beads start to make arrays. So ordering of beads take place after some time and there is ordering at a critical flow rate. After this critical flow rate clumping of beads takes place. As suction is increased further there will be no clumping and the saturation flow rate is reached where the upper injected flow rate is equal to the lower chamber suction flow rate. Hence polystyrene microbeads can be manipulated on microchannel glass either by applying pressure or flow rate. The fluid cell is made of glass. The fluid cell can also be made of plastic. As there are limitations of the plastic the fluid cell made of glass is preferred and the leakage issues are very less in glass. The fluid cells made of plastic have their importance because of its simple making from a 3D printer and are modeled by solid works.

## 2.2 Literature review

### 2.2.1 Microbeads Background

As mentioned, microbeads are microparticles which have several biotechnical applications. Micro beads are advantageous because of their size distribution and excellent spherical shape. They can be prepared from different polymers like polystyrene, polymethylmethacrylate (PMMA), polyvinyl toluene (PVT), styrene/butadiene (S/B) copolymer, styrene/vinyl toluene (S/VT). Microspheres are dyed with oil-soluble dyes, dissolved in a solvent which swells the beads.<sup>27</sup>

The solvent is then evaporated to leave the dye stranded inside the beads. The beads are permanently dyed in aqueous suspension. There are different applications, like flow cytometry, and there are different microspheres specially prepared for these applications. Fluorescent dyed microspheres, which contains excitation and emission spectra, can be chosen the ones we need. Superparamagnetic beads respond to a magnet but display negligible residual magnetism. The surface groups are intended for covalent coupling of ligands (proteins, DNA, etc.). SiO<sub>2</sub> with natural hydroxyl or silanol (Si-OH) surface groups- for adsorption of nucleotides with low protein binding.<sup>27</sup>

Sizing is an important type of particle analysis for applications in the life sciences. Establishing microsphere size allows us to predict particle behavior (movement in solution, settling time), calculate surface area available for binding, and determines best methods for handling (e.g. performance of separations). Sizing is also a useful tool for monitoring certain aspects of microsphere synthesis and modification processes.<sup>28</sup> The size distribution of beads in our thesis has a narrow size distribution and the size of beads is 4.6µm with a coefficient of variation is 6.1% and should be stored at 2 to 8 C.

Monosize polystyrene  $(C_6H_5CH=CH_2)_n$  microbeads are prepared by dispersion polymerization in different alcohol/ water media. Azobisisobutyronitrile and polyacrylic acid were utilized as initiator and steric stabilizer, respectively.<sup>29</sup> The polymerizations were performed in three kinds of dispersion media having different polarities: isopropanol/water, 1-butanol/water, and 2-butanol/water. The effects of initiator and stabilizer concentrations, alcohol/water ratio, and monomer/dispersion medium ratio on the size and monodispersity of the polymeric microbeads were investigated.<sup>29</sup>

By dispersion polymerization, polystyrene (PS) microbeads were obtained in the size range of 1.0-5.0  $\mu\text{m}$  with narrow size distribution or in the monosize form. The average size and size distribution of microbeads with increasing polarity of the dispersion medium. The average size and size distribution increased with increasing initiator concentration in all dispersion media. The increase in the stabilizer concentration in homogeneous dispersion media resulted in a decrease in average size and size distribution of the microbeads. A clear increase was observed in the average size with increasing monomer/dispersion medium ratio. Iso-propanol/water dispersion medium provided monosize microbeads with higher values of monomer/dispersion medium ratio.<sup>29</sup>

The physical equations applied for polystyrene beads are settling velocity, number of beads/gram, coefficient of variation (size distribution of the microsphere population), and settling time of beads. These equations are helpful in assessing the settling of microbeads in the fluid medium and also if the beads are not of uniform size there are chances that some beads flow through channels to lower chamber. So the size distribution is an important factor. If there is more change in size distribution of beads that can be due to different diameters of beads. The beads may settle on to channel glass by gravitation and the when suction is applied the beads

will settle depending on the different settling velocities. So settling velocity and settling time are important properties during manipulation of these beads.

The maximum settling velocity for a single microsphere (in water) is related to mean diameter and density of microbeads and is given by the equation

$$V_m = 5.448 \times 10^{-5} \cdot (\rho_s - 1) \cdot d^2$$

where  $V_m$  = maximum settling velocity (cm/sec) for a single microsphere settling in water at room temperature under the influence of normal gravitational force (1G);  $\rho_s$  = density of solid sphere ( $\text{g/cm}^3$ );  $d$  = mean diameter ( $\mu\text{m}$ )

The settling velocity is an important factor because during manipulation the beads are in suspension in a fluid environment and if the settling velocity is more then the effect of suction is overcome by settling velocity thereby making the suction or pressure factor less important.<sup>30</sup>

The settling time of microbeads depends on true settling velocity and is given as

$$t = h / V_{h5\%} \quad \text{or} \quad h / V_{ch5\%}$$

where  $t$  = settling time (sec);  $h$  = distance from top of the liquid to the bottom layer of settling solids (cm);  $V_{h5\%}$  = true settling velocity or hindered velocity (cm/sec) for a 5 % w/w suspension of microspheres settling in water at room temperature under the influence of normal gravitational force (1G);  $V_{ch5\%}$  = hindered settling velocity in the centrifuge (cm/sec) for a 5% w/w suspension of microspheres settling in water at room temperature<sup>30</sup>

The settling time is a vital factor because if we calculate the settling time of beads we can know what time it takes for the beads to settle and also we can know if they are influenced by gravitational force. The viscous nature of fluids increases the settling time. The number of microspheres per gram is proportional to the density of solid sphere and the mean diameter of spheres (polystyrene microbeads).



$$N = 6 \times 10^{12} / \pi \rho_s d^3$$

where  $N$  = # microspheres / gram for dry powders;  $\rho_s$  = density of solid sphere ( $\text{g/cm}^3$ );  $d$  = mean diameter ( $\mu\text{m}$ )<sup>30</sup>. From this we can estimate number of microspheres those can prepared in unit weight of powders.

Coefficient of variation (size distribution of the microsphere population) is indirectly proportional to mean diameter of beads.

$$CV = SD / d$$

where  $CV$  = coefficient of variation (size distribution of the microsphere population),  $SD$  = standard deviation ( $\mu\text{m}$ );  $d$  = mean diameter ( $\mu\text{m}$ )

The size distribution of microsphere population varies as the diameter of beads change. So if the beads are uniform and have same diameter then the size distribution of microspheres is uniform.<sup>30</sup>

## 2.2.2 Microchannel Glass

Microchannel glass is made of glass with channels of micro-level range. The channels are uniform throughout and these microchannel glasses have several applications in manipulation of microparticles and also optical industry. So the fabrication and characterization of a microchannel glass is discussed. The channels or capillaries are in a regular parallel array which are arranged in a two-dimensional hexagonal close packing configuration with diameter of channels is about 4-5  $\mu\text{m}$ . The microchannel glass is used as mask for massively parallel patterned lithographic applications. Microchannel glass has high packing density with channel diameters as small as of a few microns. In a typical array the number of channels is greater than  $10^6$  and excellent control is maintained over the geometric regularity in the placement of channel positions as well as the depth of channel formation.

The fabrication of microchannel glass is obtained by a draw process. The microchannel glass arrays are prepared by arranging dissimilar glasses, of which at least one glass type is usually acid etchable, in its predetermined configuration. Construction of array starts by insertion of a cylindrical acid-etchable glass rod (channel glass) into an inert glass tube (matrix glass) as shown in the Figure 2.1.1 The pair is then drawn at high temperature under vacuum to reduce the overall cross section to that of a fine filament shown in Figure 2.1.2. The filaments are then stacked in a bundle, refused and redrawn until appropriate channel diameters and desired number of array elements are achieved shown in Figure 2.1.3. Interdiffusion of the two glass materials at elevated temperatures will cause a reduction in shape of channel after etching.<sup>31</sup>

The sample becomes a homogeneous glass after repeated exposures to elevated temperatures as shown in Figure 2.1.4. The center-to-center spacing of the rods and their diameters in the finished product become independently adjustable parameters, by adjusting

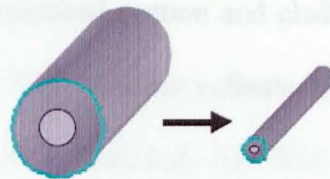
the ratio of the diameter of the etchable glass rod to that of outside dimension of the inert glass tubing. The channel glass has a relatively low absorption coefficient in the visible portion of the spectrum. The low optical absorption coefficient is an important consideration for optical characterization of quantum confined materials deposited into the channels, as well as for its potential use in electro-optic device applications. The circumference of the channel glass array structure was added by an inert glass cladding at the final draw to protect the array edge and at later stages to act as a support structure for characterization.<sup>31</sup>

**Microchannel glass is fabricated by bundling composite glass fibers into a hexagon and drawing the bundle at elevated temperature.**

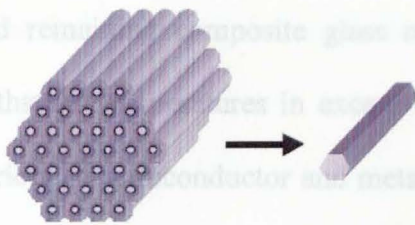
1. Etchable glass rod is inserted into etch-resistant glass tube.



2. The nested rod and tube are drawn at elevated temperature to a fiber.



3. Fibers are bundled, clamped, and drawn into a hexagonal fiber.



4. Hexagonal fibers are stacked in a 12-sided bundle and fused in a glass cladding under vacuum.



**NCG can be made by stretching a microchannel glass boule to a taper.**

Figure 2.1 Fabrication process of Microchannel glass<sup>32</sup>

When the fabrication is complete, the channel glass is cut perpendicular to the direction of channels to get about 0.5 to 5 mm sections of material. Then the ends of the sections are ground with diamond compound and final polished to an optical flat with 0.5 $\mu$ m diamond powder. Channel glass is then etched with a hydrochloric acid solution in water, after a thorough cleaning with methanol to remove any surface contamination. After the etching process, the samples were rinsed in distilled water, followed by a methanol rinse and then dried. The spatial measurements on geometry and regularity of channel diameters in the array were made with scanning electron microscope. After that channel glass is gold sputtered to prevent it from charging during SEM operation. SEM micrograph basically shows hexagonal close packing arrangement of channels after acid etching. Etched portion was crumbled by a gentle tapping of the sample and become separated from unetched portion and cladding. The dark regions are bottom of the etched channels and the light regions indicate sections of unetched glass. Samples were durable when they were fine annealed, and then they are polished and etched as done earlier.<sup>31</sup>

Hence ultra thin sections of channel glass can be made, as the stress within the etched and remaining composite glass material is relieved by annealing. The channel glass can withstand temperatures in excess of 600 $^{\circ}$ C without deformation. Therefore it is suited for a variety of semiconductor and metal-deposition processes. They can be deposited into channel glass by metal organic chemical vapor deposition, which requires temperatures over 400 $^{\circ}$ C. The channel glass has other applications such as lensing and collimating of neutral beams like x-rays and neutrons.<sup>31</sup>

The Microchannel glass has a composite glass structure, high aspect ratio (2000:1), uniform and parallel channels. It is etchable glass that can be removed with acid and has channels diameter ranging from  $\sim$ 200nm to  $\sim$ 5 $\mu$ m. It is thermally stable upto  $\sim$ 1000 C and its

packing density is  $\sim 10^9/\text{cm}^2$ . It contains  $\sim 10^6$  pores. The glass can be cut, ground and polished to desired size and shape.

Microchannel glass technology enables connections to millions of neurons and it has excellent compatibility with biological tissue. Its shape can be made to conform to curvature of any neural surface. Metal can be deposited in hollow channels to provide a uniform array of millions of metal electrodes. Microelectrodes offer micron-scale spatial resolution<sup>32</sup>

### 2.2.3 Microchannel Plate technology

The Microchannel glass is different from microchannel plate. However the principle of fabrication and the use of microchannel plate are similar to that of microchannel glass. The basic steps used to obtain the unprocessed microchannel plate are given as follows. Single channels are drawn as solid-glass fibers having two components, a core glass, soluble in a chemical etchant, and a lead glass cladding which is not soluble in the core glass etchant. The fibers from the first draw are packed together in a hexagonal array, and drawn again into hexagonal multi-fibers. The latter are stacked again and fused within a glass envelope to form a boule. This boule is then sliced, often at a small angle ( $8^\circ$ - $15^\circ$ ) from the normal to the channel axes; the resulting wafers are then edged, beveled and polished into a thin plate.<sup>33</sup>

### 3. Experimental Setup

#### 3.1 Introduction

The manipulation of polystyrene microbeads on microchannel glass is performed in a fluid cell. The fluid cell is basically a two-chambered cell made of glass slides. The two-chambered fluid cell, a syringe pump and an optical microscope make up the experimental setup. This mentioned experimental setup is for manipulation of beads when automated flow rate is applied. If the manipulation of beads is performed by applying pressure then the experimental setup consists of two chambered fluid cell, wooden block with syringes suspended in the block, weights for suspension or being held on syringes, and an optical microscope. In fluid cell the glass slides are made to put in such a way that we get two chambers one above the other separated by a hole. The hole is covered by an etched microchannel glass. The building of fluid cell is a difficult task as there should not be any leakage after it is sealed. The microchannel glass in the fluid cell is the source where the manipulation of microbeads can be done. Manipulation of bulk quantity of beads in a fluid cell is very difficult and so the design of fluid cell is very important and is a challenging point in the experimental setup. The glass slides are cut into thin slides with a diamond pen and they can be used as spacers for building the chambers of the fluid cell. The spacers are attached to glass slide with either epoxy or silicone. Then a hole is drilled on one glass slide which is separator of two chambers. After the spacers are kept as walls of chamber we make outlets for the flow into fluid cell. The outlets are connected by polyvinyl chloride (PVC) microtubes which are inturn connected to syringes. The etched microchannel glass is placed on the drilled hole and glued on the outer area with silicone or epoxy. Then the chamber is sealed by a glass slide. The fluid cell top view and front view is shown in figure. The fluid cell then can be used for manipulation of beads by applying pressure or flow rate.

### 3.2 Microchannel Glass sample preparation

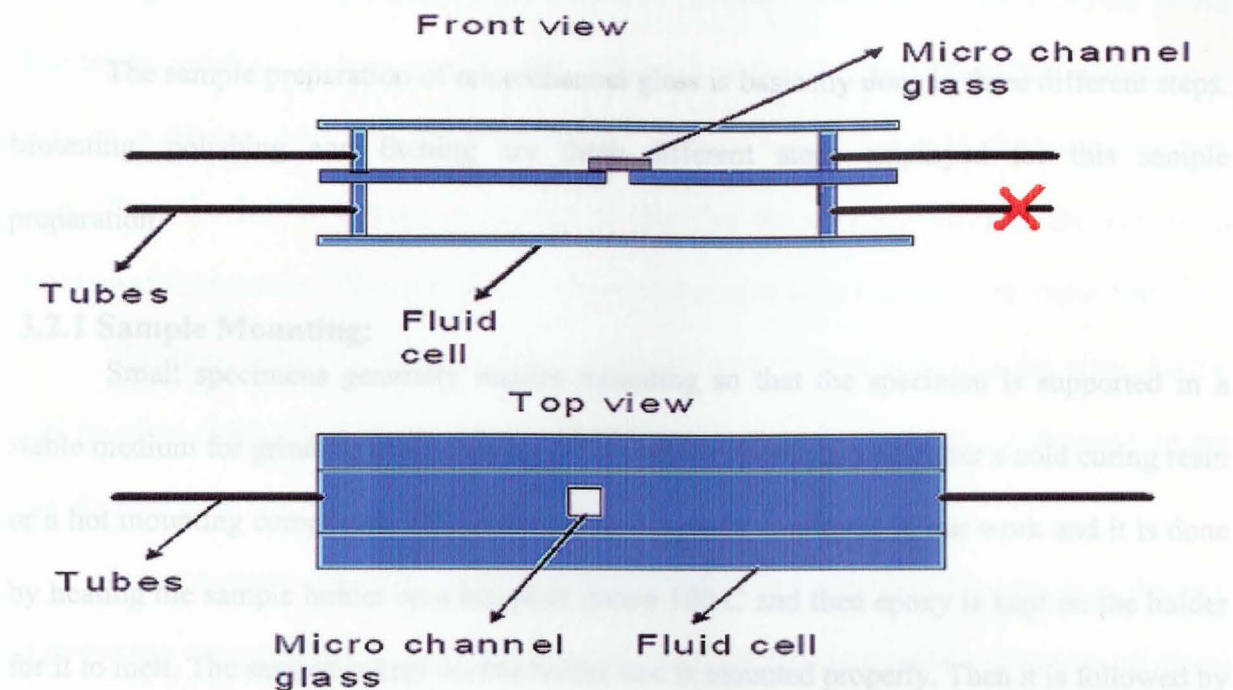


Figure 3.1 Top view and front view of Fluid cell model

As mentioned the channel glass, after etched, is kept on the drilled hole of the two-chamber glass fluid cell. The tubes at the outlets of chambers are connected to syringes from where we can pass the beads solution with the help of syringe pumps. The four outlets are used effectively for their purposes respectively. The syringe pump is used effectively in varying the flow rates. The injected flow rate in upper chamber is equal to the total of flow rates suctioned in lower chamber and upper chamber. So the suction flow rates in lower chamber is varied along with the suctioned flow rate in upper chamber keeping injected flow rate at a constant value. Then experiment is repeated with different injected flow rate.

## 3.2 Microchannel Glass sample preparation

The sample preparation of microchannel glass is basically done in three different steps. Mounting, polishing and Etching are three different steps employed for this sample preparation.

### 3.2.1 Sample Mounting:

Small specimens generally require mounting so that the specimen is supported in a stable medium for grinding and polishing. The medium chosen can be either a cold curing resin or a hot mounting compound. Hot mounting technique is employed in our work and it is done by heating the sample holder on a hot plate above 100 C and then epoxy is kept on the holder for it to melt. The sample is kept on this holder and is mounted properly. Then it is followed by polishing.

### 3.2.2 Polishing

Polishing is the most important step in preparing a specimen for micro structural analysis. It is the step which is required to completely eliminate previous damage. Polishing processes using extremely fine spherical silica particles produce deformation-free surfaces. Final polishing abrasives are selected based upon specimen hardness and chemical reactivity. The most common polishing abrasives are alumina and colloidal silica. Alumina abrasives are primarily used as mechanical abrasives because of their high hardness and durability. Colloidal silica's are relatively soft final polishing abrasives with a high chemical activity. They are ideal for chemical mechanical polishing.<sup>34</sup>

Generally polishing is done in two steps. Coarse polishing and then fine polishing are the steps employed.



### 3.2.2a Polishing methods

In general, coarse polishing is performed on grinding wheel and abrasive papers. In our experiment polishing is done on 400, 600, 1200 grit abrasive papers. Then fine polishing is done on polishing cloth with diamond powder of sizes 6-4, 4-2, 1-0.25, 0.25-0  $\mu\text{m}$  in that order. Then the holder is kept in acetone to dissolve the crystal bond and the sample is unmounted from holder. Then it is dipped in iso-propanol to keep it clean from impurities.

The same polishing steps are repeated on the other side of microchannel glass. So the final polished (both sides) microchannel glass should be etched to open up the channels all the way through from one side to the other.

In our research the microchannel glass is polished by coarse polishing initially. But due to impurities during polishing on grit papers, these grit papers are avoided and coarse polishing is done on polishing cloth with water spread on it. Then channel glass is polished on polishing cloth with diamond powder of sizes 6-4, 4-2, 1-0.25, 0.25-0 $\mu\text{m}$  in that order, with water mixed along with diamond powder and spread on the polishing cloth. The polishing of microchannel glass is done until it gets a mirrored look without any inclusions or dents or scratches. Then as mentioned it is kept in acetone to unmount the sample from the holder. Then it is cleaned in Iso-propanol. The channel glass is polished on the other side by mounting it in a similar way we did on the other side. Then channel glass is taken for etching.

### 3.2.3 Etching

Etching is defined as the process to reveal structural details by preferential attack of a metal surface with an acid or a basic solution. Etching time is very important for the channels to open up such that suction can be applied easily and the beads can be manipulated on the microchannel glass. If the etching time is more then the sample is more etched and it may destroy the sample. If etching time is less then the channels in microchannel glass won't open

up. Several compositions of etchants have several etching times. The compositions of etchant are varied by changing the parts by volume of Nitric acid used in the etchant. For 100 parts of pure water 1 part glacial acetic acid and 0.1 parts Nitric acid the etchant time is about 15 hrs. When it is 0.5 parts nitric acid then etching time is 12 hrs. When it is 0.01 part nitric acid the etching time is 9 hrs. However 0.1 part nitric acid composition is better suited as the channels are opened up and etching is done properly. So we used the composition of 100 parts water, 1 part glacial acetic acid and 0.1 part nitric acid.

Etching process is done in a setup where the sample is suspended in an etchant in a glass beaker with a stirrer as shown in Figure 3.3. Etching time is about 15 hrs. So the beaker is kept on the stirrer plate for about 15 hrs to get proper etching. The etchant used is 100 ml water, 1ml glacial acetic acid, 0.1 ml nitric acid. The glass slides hold the microchannel glass firmly so that there is flow all through the channels and channels open up after etching.

Figure 3.3 Etching setup for Microchannel glass

The etched microchannel glass looks like the figure 3.4 shown below. It shows a SEM of microchannel glass taken at 1500X magnification and at a voltage of 25kV. The channels are about 4-5µm in diameter as calculated from scale which also matches with the given value. The channels are etched all the way through other side. Hence the channels are open and the manipulation can be done by applying suction. If etching is not done properly the channels cannot open up and the manipulating the beads is very difficult.

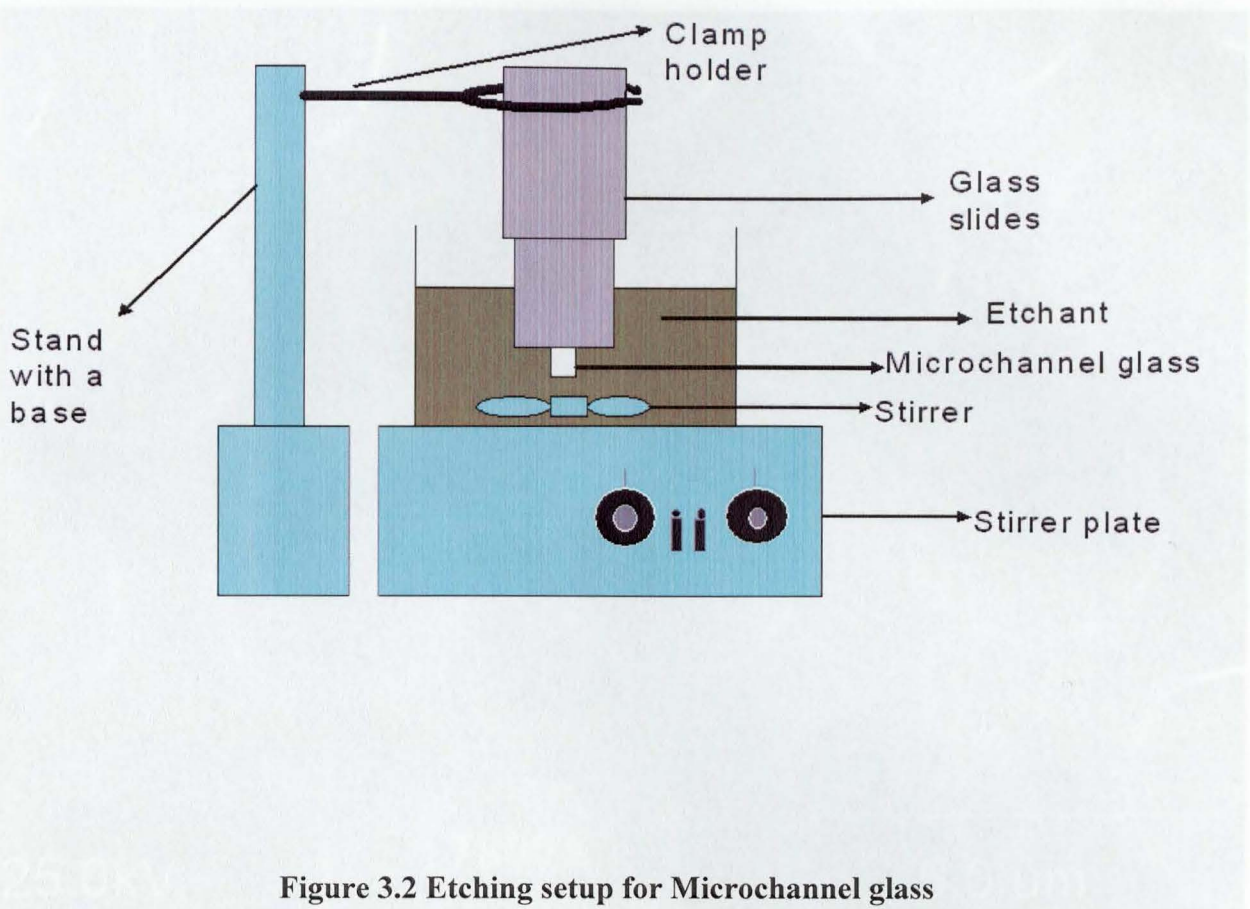


**Figure 3.2 Etching setup for Microchannel glass**

The etched microchannel glass looks like the figure 3.4 shown below. It shows a SEM of microchannel glass taken at 7800X magnification and at a voltage of 25kV. The channels are about 4-5 $\mu$ m in diameter as calculated from scale which also matches with the given value. The channels are etched all the way through other side. Hence the channels are open and the manipulation can be done by applying suction. If etching is not done properly the channels cannot open up and the manipulating the beads is very difficult.

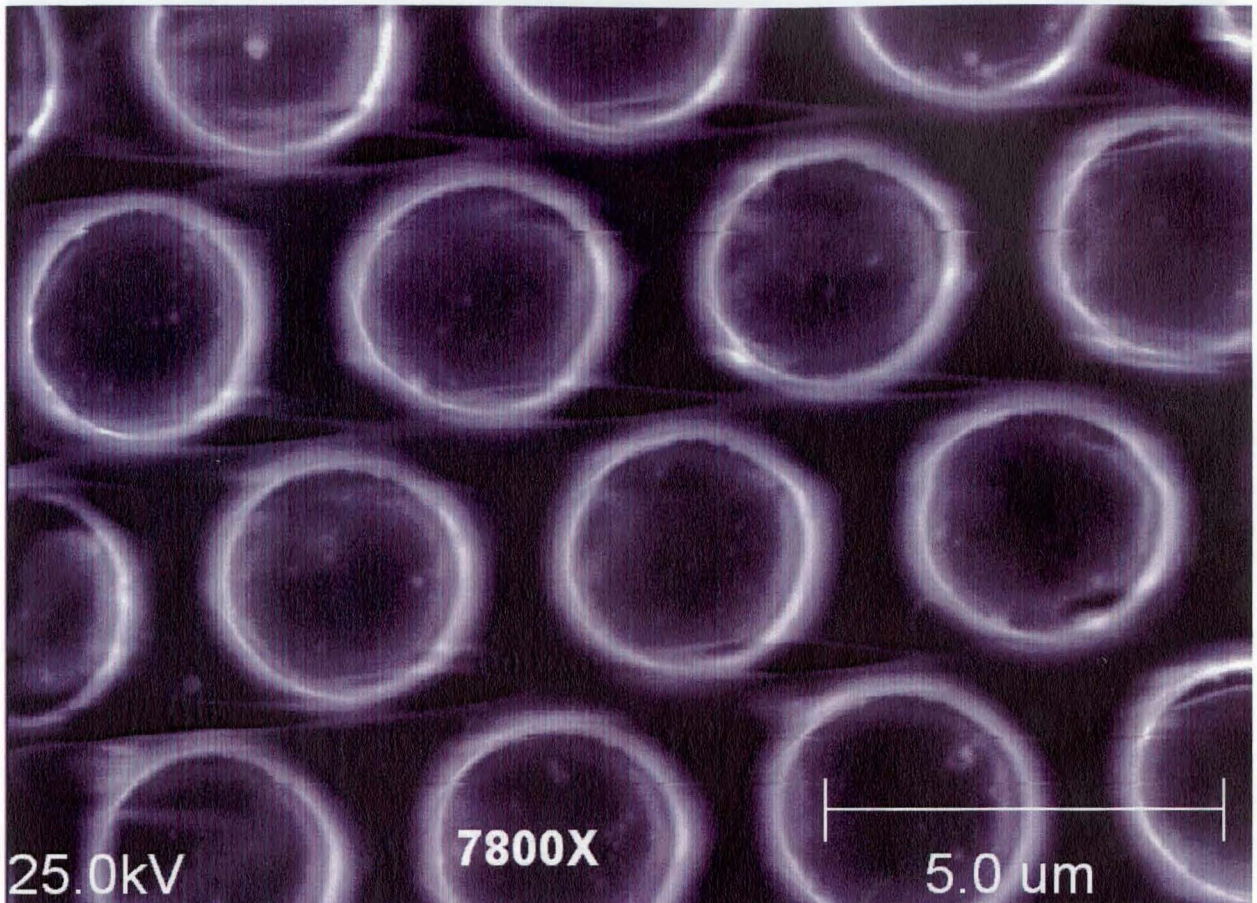


**Figure 3.3 SEM micrograph of Microchannel glass at 7800X magnification and 25 kV**

Figure 3.4 SEM micrograph of microbeads at 3000X magnification and 8 kV

#### Figure 3.5

The microbeads used in this thesis are basically polymeric in nature. The microbeads are prepared from polystyrene and some beads are magnetic in nature because of iron oxide present in it. It is evident from the spectrum that Iron (Fe) is present in it. This is the spectrum obtained from EDS during operation of SEM of microbeads. The peak highest in the spectrum is occupied by Fe. So microbeads are paramagnetic in nature and there are several applications of its paramagnetic nature. The paramagnetic nature is mainly useful when the magnetic manipulation is employed for separation of biological cells, proteins from the beads.

Figure 3.5 Spectrum of Microbeads from EDS

Figure 3.5 Spectrum of Microbeads from EDS

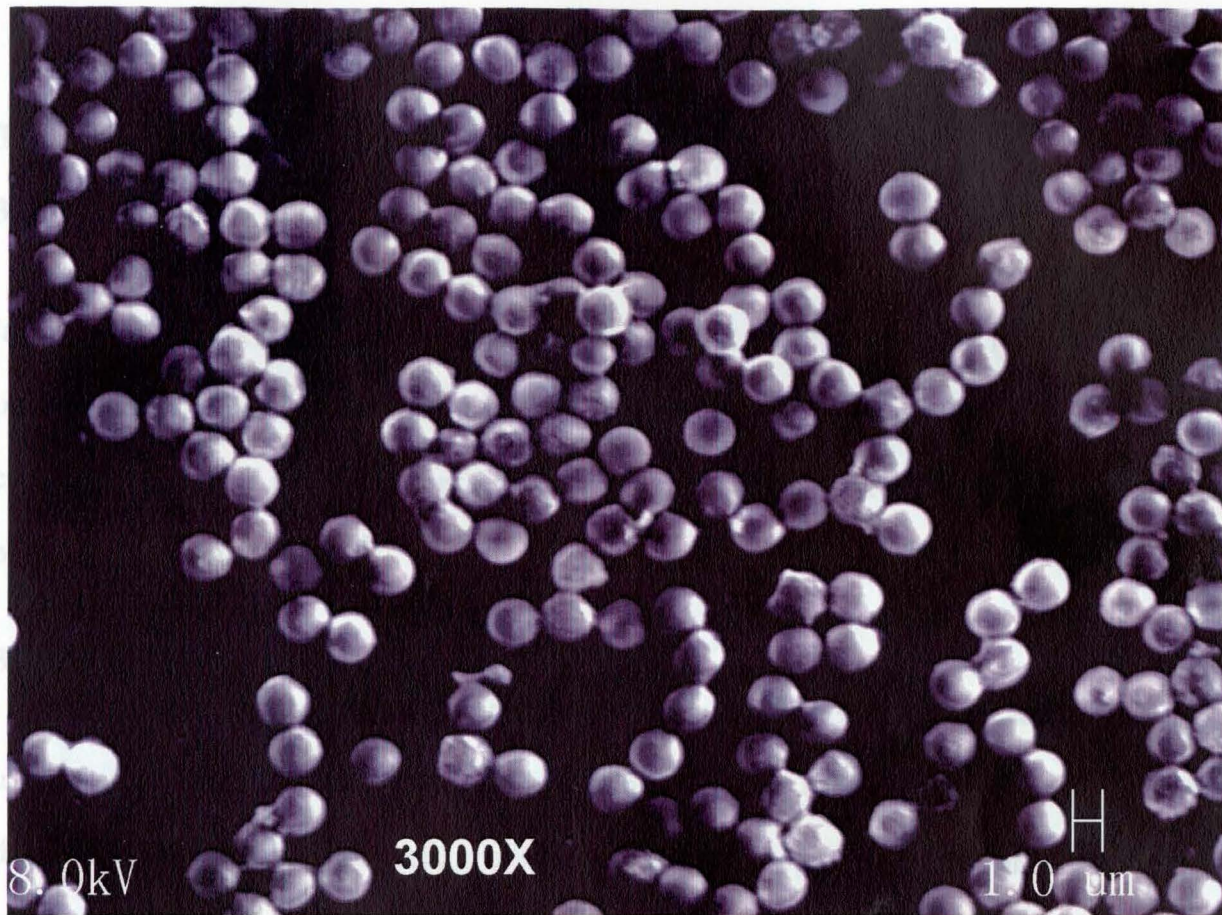


Figure 3.4 SEM micrograph of microbeads at 3000X magnification and 8 kV

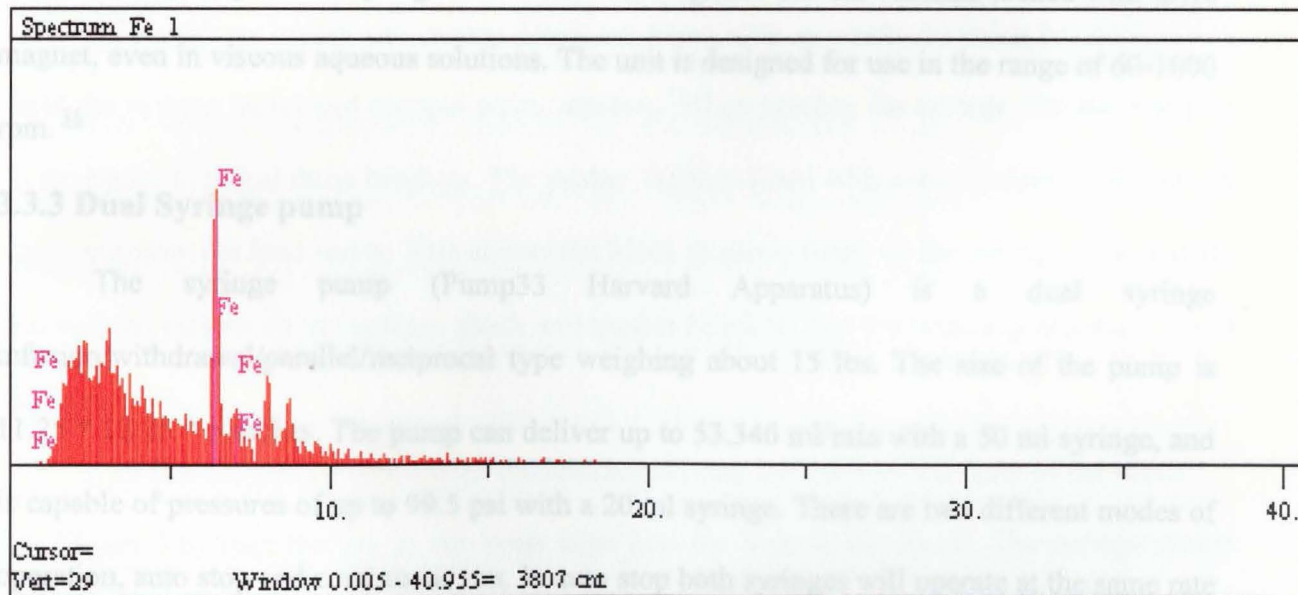


Figure 3.5 Spectrum of Microbeads from EDS

### 3.3 Equipment used

#### 3.3.1 Hot plate

The Model HPA1900 hot plates are general purpose heating devices intended for laboratory procedures requiring temperatures from 38°C (100°F) to 371°C (700°F). The top plate is heated by a resistance heater embedded in a refractory material. The plate is made of cast aluminum to aid in uniform surface temperature. The temperature of the plate is controlled by a bimetallic thermostat. <sup>35</sup>

#### 3.3.2 Stirring plate

The stirring plate is used during etching process of microchannel glass where the setup is kept on stirring plate and its purpose is stirring, such that constant flow through channels during etching is maintained. Stirrer plate can also be used for the preparation of culture media, acid-based titrations requiring constant temperature and for the slow stiffening of culture media. Strong magnetic coupling ensures that the magnetic stir bar remains locked with drive magnet, even in viscous aqueous solutions. The unit is designed for use in the range of 60-1000 rpm. <sup>36</sup>

#### 3.3.3 Dual Syringe pump

The syringe pump (Pump33 Harvard Apparatus) is a dual syringe infusion/withdrawal/parallel/reciprocal type weighing about 15 lbs. The size of the pump is 11.25 \* 12.25 \* 6 inches. The pump can deliver up to 53.346 ml/min with a 50 ml syringe, and is capable of pressures of up to 99.5 psi with a 20 ml syringe. There are two different modes of operation, auto stop and continuous run. In auto stop both syringes will operate at the same rate and will stop when either syringe reaches a limit stop. In continuous run, with both syringes operating at the same rate, the pump automatically reverses the direction of travel for both the

syringes, when the end of travel is reached. In proportional mode, the pump operates as in auto stop, but independent rates and diameters are set for each syringe. The syringes may pump either in the same direction (parallel) or in opposite directions (reciprocal).<sup>37</sup>

### 3.3.3a Loading Syringes

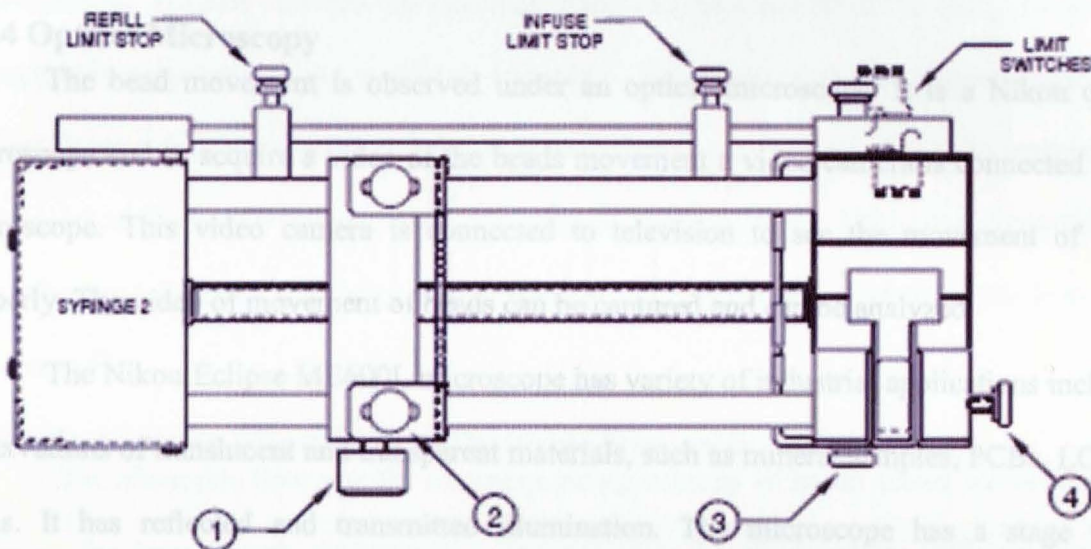


**Figure 3.6 loading of syringes on syringe pump<sup>37</sup>**

The syringe holder and pusher block are fitted with movable retaining brackets which hold the syringe barrel and plunger when refilling. When loading the syringe into the pump, it is necessary to adjust these brackets. The pusher block is fitted with a mechanism to release the drive nut from the lead screw. This allows the block to move freely so the syringe to be loaded. Loosen the screws on the syringe block and pusher block to free the retaining brackets (2 and 3, Figure 3.6).

To free the pusher block from the lead screw, turn the knob on the front of the block (1, Figure 3.6) until the pin in the knob slips into the hole in the block. The syringe clamp locking screw on the right side of the syringe block (4, Figure 3.6) should be loosened and the clamp rotated to the side. Place the syringe barrel on the syringe holder block and move the

pusher block to accommodate the plunger. Syringe clamp is rotated and pressed down firmly on the syringe barrel. It is then secured in place by tightening the locking screw (4, Figure 3.6). Then the fluid cell is kept under the optical microscope after syringes are loaded and connected to outlets of fluid cell through tubes.

### 3.3.4 Optical Microscopy

The bead movement is observed under an optical microscope. It is a Nikon optical microscope and to acquire a video of the beads movement a video camera is connected to the microscope. This video camera is connected to television to see the movement of beads properly. The video of movement of beads can be captured and can be analyzed.

The Nikon Eclipse ME600L microscope has variety of industrial applications including observations of translucent and transparent materials, such as mineral samples, PCBs, LCDs or films. It has reflected and transmitted illumination. The microscope has a stage where specimen can be kept. The objective lenses have adjusting knobs so that we can change the contrast and focus the image in better way. Light can interact with a specimen through a variety of mechanisms to generate image contrast. These include reflection from the surface, absorption, refraction, polarization, fluorescence, and diffraction.<sup>38</sup>

It has a 60mm par focal distance and larger objective diameter and provides both longer working distances and higher numerical apertures. The microscope stand incorporates a built-in light source for diascopic illumination and an episcopic/diascopic changeover switch for transparent and translucent materials. The depth of field is the thickness of the specimen that is acceptably sharp at a given focus level. In contrast, depth of focus refers to the range over which image plane can be moved while an acceptable amount of sharpness is maintained.<sup>38</sup>

The diameter of the field in an optical microscope is expressed by the field-of-view number, or simply the field number, which is the diameter of the view field in millimeters measured in the



intermediate image plane. In most cases, the eyepiece field diaphragm opening diameter determines the view field size. Microscope objectives are generally designed with a short free working distance, which is defined as the distance from the front lens element of the objective to the closest surface of the coverslip when the specimen is in sharp focus. The parfocal length represents the distance between the specimen plane and the shoulder of the flange by which the objective is supported on the revolving nosepiece. Three critical design characteristics of the objective set the ultimate resolution limit of the microscope. These include the wavelength of light used to illuminate the specimen, the angular aperture of the light cone captured by the objective, and the refractive index in the object space between the objective front lens and the specimen.<sup>39</sup>

### 3.3.5 To Find the Allowable and Desirable Flow rates

The allowable flow rate for a corresponding velocity of beads across the microchannel glass or for flow through channels in a channel glass is calculated for different theoretical values of the flow rate. In the fluid cell if we consider the values shown in figure 3.7 then we can calculate the allowable or desirable flow rates.

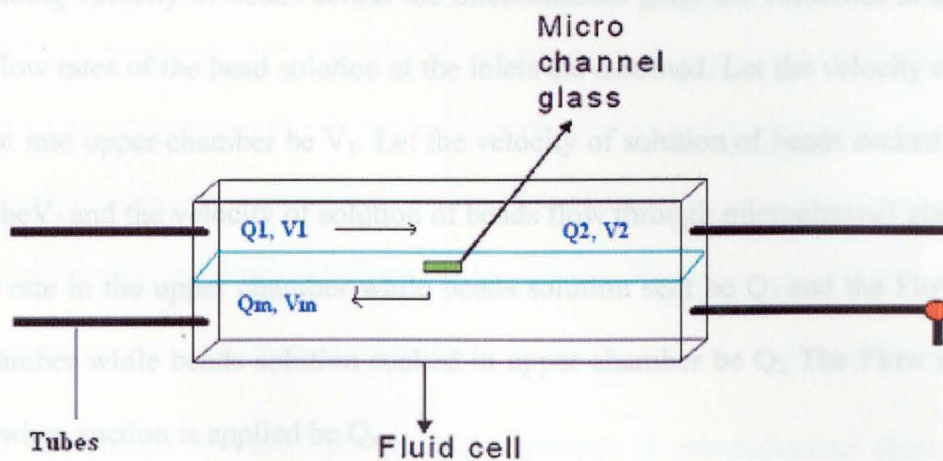
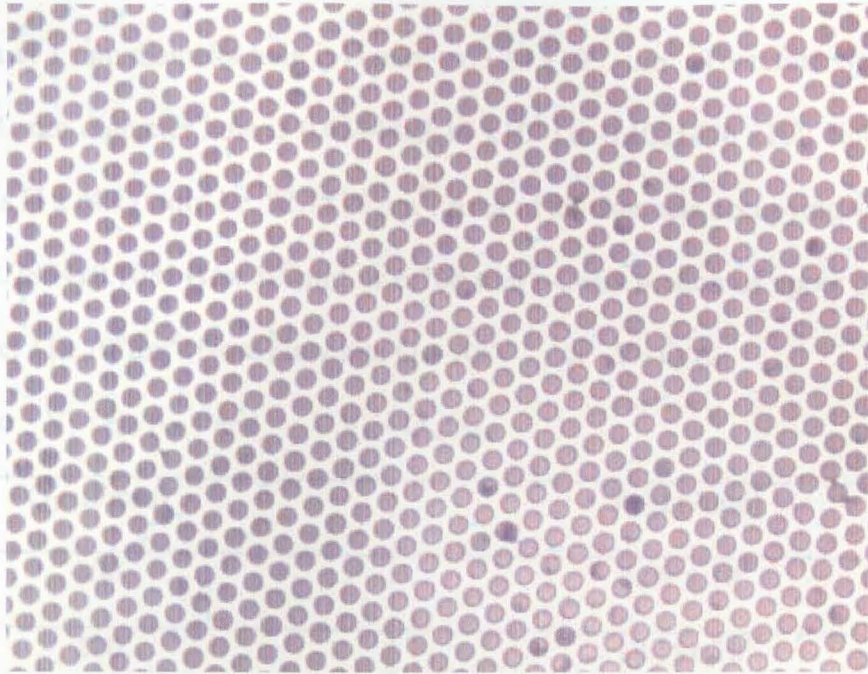


Figure 3.7 The Fluid cell setup with Different flow rates and velocities at outlets



**Figure 3.5 Microchannel glass with average field count 1025**

The theoretical values of flow rates for a corresponding velocity of beads through microchannels are calculated by calculating for a given values of flow rates to calculate the velocity of beads solution at the inlets. In order to find the allowable flow rate for a corresponding velocity of beads across the microchannel glass the velocities at the inlets and also the flow rates of the bead solution at the inlets are assumed. Let the velocity of solution of beads sent into upper chamber be  $V_1$ . Let the velocity of solution of beads sucked in the upper chamber be  $V_2$  and the velocity of solution of beads flow through microchannel glass is  $V_m$ . Let the Flow rate in the upper chamber while beads solution sent be  $Q_1$  and the Flow rate in the upper chamber while beads solution sucked in upper chamber be  $Q_2$  The Flow rate in lower chamber when suction is applied be  $Q_m$

$$\text{Flow rate } Q = \text{cross sectional Area } A \times \text{velocity } V \quad \mu\text{l/min}$$

At a magnification of 400X (40X objective) image the number of channels is found to be 1025. The field area of the channels is  $29760.8 \mu\text{m}^2$ . Hence No. of channels / unit area is

1025/29760.8 i.e., 0.03444 per  $1\mu\text{m}^2$  area. Now the no. of channels in 1 mm diameter hole is  $(\Pi \times 1 \times 1)$ . Area of 1 mm diameter hole is  $\Pi \text{ mm}^2$  or  $3.14 \times 10^6 \mu\text{m}^2$ . Therefore No. of channels in an area of 1 mm diameter hole is  $0.03444 \times 3.14 \times 10^6$  i.e.  $0.1081416 \times 10^6$ . Now the area of each channel is  $\Pi \times (4.1)^2 \mu\text{m}^2$  i.e.  $52.7834 \mu\text{m}^2$ . Area of all channels occupying 1mm diameter hole ( $A_m$ ) =  $52.7834 \times 0.1081416 \times 10^6 \mu\text{m}^2$  or  $6.708 \text{ mm}^2$ . Cross section of upper chamber is  $11 \text{ mm} \times 1 \text{ mm}$  i.e.  $11 \times 10^6 \mu\text{m}^2$ . Now Flow rate  $Q = A \times V$  or  $V = Q/A$

Hence we have  $V_1 = Q_1/A_1$  and  $V_m = Q_m/A_m$

$Q_1(\mu\text{l}/\text{min})$	$V_1(\mu\text{m}/\text{min})$
100	$9.09 \times 10^3$
200	$18.18 \times 10^3$
300	$27.27 \times 10^3$
400	$36.36 \times 10^3$

**Table 3.1 the Inlet flow rate as against velocity of beads flow**

$Q_m(\mu\text{l}/\text{min})$	$V_m(\mu\text{m}/\text{min})$
50	$8.76 \times 10^3$
100	$17.519271 \times 10^3$
150	$26.28 \times 10^3$
200	$35.038 \times 10^3$

**Table 3.2. Tabulation of Flow rate through channels of microchannel glass as against velocity of beads through channels.**

The tables 3.1 and 3.2 show the allowable velocity of flow of beads solution in upper chamber and through microchannel glass in accordance with the flow rates applied.

### 3.4 Challenges in making Fluid Cell

The design of fluid cell is the crux of the process. If it is not done properly then the whole process is ruined. There are challenges in designing Fluid cell because of working with glass and leakage problems as thin slip glass cannot withstand high pressure. The glass slides which are cut into thin slides with a diamond pen are used as spacers for building chambers of fluid cell. The spacers are attached with a silicone to glass slide which has a drilled hole. The drilled hole on one glass slide acts as a separator of two chambers. The spacers are kept as walls of chamber and outlets for the flow into fluid cell connected by polyvinyl chloride (PVC) microtubes which are inturn connected to syringes. The etched microchannel glass is glued onto the drilled hole applying silicone on outer area of microchannel glass. Then the chamber is sealed by a glass slide. We tried manipulating microbeads by sending them into the cell and sometimes there is leakage due to uneven placement of spacers. Sometimes the glass breaks due to very high pressure created in the chamber. So an alternate solution for the design of fluid cell is discussed.

Figure 3.6 Solid works design of the fluid cell model.

As mentioned, the fluid cell is a two chambered glass cell made of glass with four outlets and the chambers are interconnected by a microchannel glass on a drilled hole. The practical difficulties like cutting of glass slides, leakage problems and handling of fluid cell with glass made us to make the fluid cell by plastic. The design of the fluid cell is modeled in solid works and is manufactured by 3D printer machine. The 3D models are made. The design of solid works is as shown in Figure 3.6. The fluid cell is made in such a way that it is identical on both sides. The fluid cell is manufactured from solid works 3D model machine. The fluid cell is made by 3D printer machine and made it to dry with a drier. It is kept vertically.

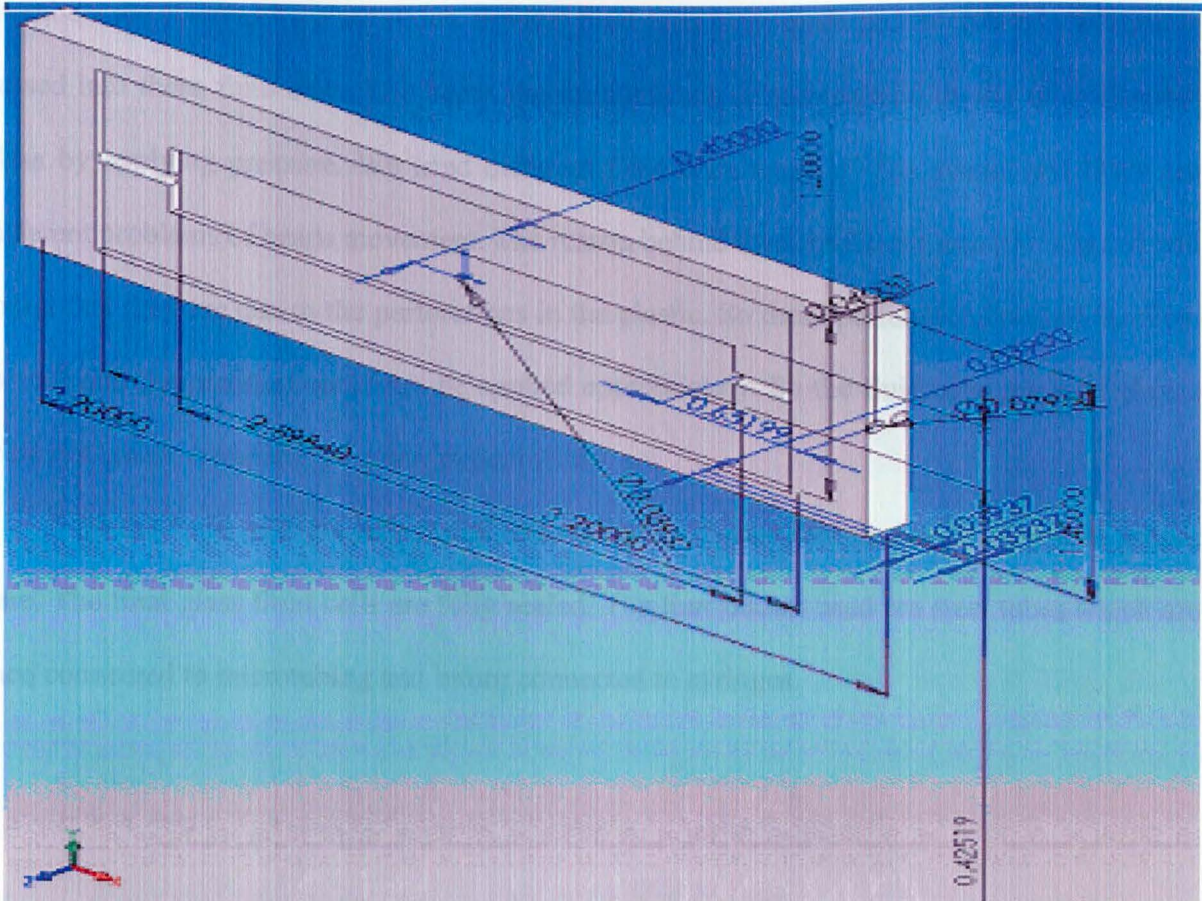


**Figure 3.6 Solid works design of the fluid cell model.**

As mentioned, the fluid cell is a two chambered glass cell made of glass with four outlets and the chambers are interconnected by a microchannel glass on a drilled hole. The practical difficulties like cutting of glass slides, leakage problems and building of fluid cell with glass made us to make the fluid cell by plastic. The design of the fluid cell is modeled in solid works and is manufactured by 3D printer machine out of which the 3D models are made. The design of solid works is as shown in Figure 3.3. This solid works model fluid cell is made in such a way that it is identical on both sides. The plastic fluid cell, after manufactured from solid works 3D model machine, has to be cured by dipping it into acetone for 20 seconds and made it to dry with a drier. It is kept overnight and it can be used for our experiment. The two

chambers are covered by glass slides. Several fluid cells were made and microbeads solution is passed into these fluid cells. The beads are immobilized or manipulated on the microchannel glass by applying pressure. We tried different fluid cells made of this plastic and there are different problems of beads movement. The reason behind these problems was investigated and found that they are due to the perforations in the plastic. So these perforations caused the flow to stall and the pressure could not be applied appropriately. So the fluid cells made of plastic were not considered further for our experiments.

So the fluid cells are redesigned and are made of glass, but in a better way with proper care. The final glass fluid cells are fully sealed. The four outlets used are steel tubes which are then connected to microtubing and inturn connected to syringes.

- i) Applying flow rate automated with the help of syringe
- ii) Applying pressure on microbeads in fluid cell

The both modes of manipulation of beads in microfluidic glass have to be performed carefully such that beads make an array when a critical flow rate and critical pressure is applied. Some precautions are to be taken while performing experiments.

## 4. Experiments

### 4.1 Experimental Procedure

The experiment is basically the manipulation of microbeads on microchannel glass by injecting the microbeads into the fluid cell. The natrosol is added to microbead solution such that the viscous nature of the solution is increased and Sodium n-dodecyl sulphate (soap solution) is added to reduce the sticking of beads. Microchannel glass after etching is cleaned with acetone. It is then placed on drilled hole of fluid cell and sealed on outer sides of microchannel glass with silicone. The experiment should be done in a clean environment in order to avoid clogging in tubes and care should be taken that fluid cell is sealed properly to avoid leakage. If there is any leakage, then applying pressure or flow rate is difficult during manipulation of beads. There are two modes of manipulation of microbeads on microchannel glass in this thesis. The manipulation of microbeads is performed by

- i) Applying flow rate automated with the help of syringe.
- ii) Applying pressure on microbeads in fluid cell

The both modes of manipulation of beads on microchannel glass have to be performed carefully such that beads make an array when a critical flow rate and critical pressure is applied. Some precautions are to be taken while performing experiments.

## 4.2 Precautionary measures

The fluid cell should be kept clean. The tubes should be kept away from impurities as they can cause clogging in the system. The beads usually stick together. Hence the beads solution is kept in an ultrasonic cleaner for some time and then is injected into chamber. The silicone is applied on glass to seal the fluid cell perfectly without any leakages. It is also preferable to test the components for free flow before attaching them to the other. For example, testing the syringe first, next testing the syringe together with the tubing and last the entire tubing/needle setup at a time. The experiment with syringe pump is performed in continuous way so that the beads solution is flowing on the microchannel glass constantly. When applying weights during the mode of manipulation by applying pressure the weights should be suspended well and also they should be placed well without falling from syringes.



### 4.3 Manipulation of beads by applying flow rate

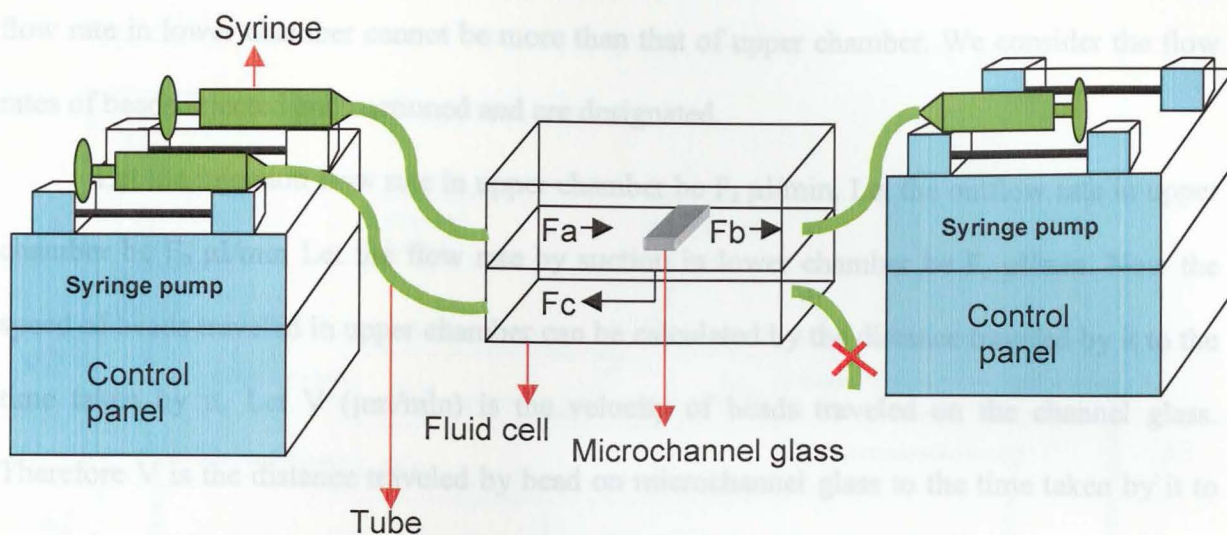


**Figure 4.1 Experimental setup of fluid cell and syringe pump**

The fluid cell is connected to the syringe pump as shown in figure 4.1. The figure shows the top view of fluid cell connected to a syringe pump. The outer ends of fluid cell with steel tubes are connected to syringes held on syringe pump through PVC tubing. The three outlets are connected to syringes. The fourth outlet is sealed to create suction in lower chamber. The microbeads solution is sent into upper chamber with syringe pumps running. Microbeads solution has a composition of microbeads, 1% natrosol and Sodium n-dodecyl sulphate (soap solution). The microbeads solution inflow rate is typed on syringe pump and also the out-flow rate. The suction flow rate is also typed on the syringe pump. Then the flow rates are changed accordingly and the beads were immobilized on the microchannel glass. The beads, with initial flow rates where suction flow rate is less, would move without any immobilization and there is some flow on channel glass. When the suction flow rate increases we will get to a point where the beads are placed in channels in a perfect array. Further increase of suction flow rate would make the beads to clump. The point where the beads make an array is the critical point and the corresponding flow rate is critical flow rate. The area above the critical point is the area where

clumping of beads is taking place. The point beyond the critical clumping is not possible as the flow rate in lower chamber cannot be more than that of upper chamber. We consider the flow rates of beads injected and suctioned and are designated.

Let the injection flow rate in upper chamber be  $F_a$   $\mu\text{l}/\text{min}$ . Let the outflow rate in upper chamber be  $F_b$   $\mu\text{l}/\text{min}$ . Let the flow rate by suction in lower chamber be  $F_c$   $\mu\text{l}/\text{min}$ . Now the speed of beads traveled in upper chamber can be calculated by the distance traveled by it to the time taken by it. Let  $V$  ( $\mu\text{m}/\text{min}$ ) is the velocity of beads traveled on the channel glass. Therefore  $V$  is the distance traveled by bead on microchannel glass to the time taken by it to travel that particular area.  $F_a$ ,  $F_c$ ,  $F_b$  values are in  $\mu\text{l}/\text{min}$  units. The flow rates  $F_a$  is kept at a constant value and the value of  $F_c$  is changed which implies changing of  $F_b$  as well. Therefore we get values of  $F_c$  at a particular  $F_a$  and this process is repeated by changing  $F_a$  and the  $F_c$  flow rates are varied until a critical flow rate  $F_c$  is obtained. The velocity of beads is calculated at that particular critical flow rate. For every critical flow rate we obtain a velocity of the bead  $V$ . The velocity of beads at critical flow rate  $F_c$  is plotted against flow rate  $F_a$ . The values of  $F_a$ ,  $F_c$  and  $V$  values are tabulated and the resulting plots of  $F_a$  vs  $F_c$  and  $V$  vs  $F_a$  is discussed in chapter 5.

#### 4.4 Manipulation of beads by applying pressure

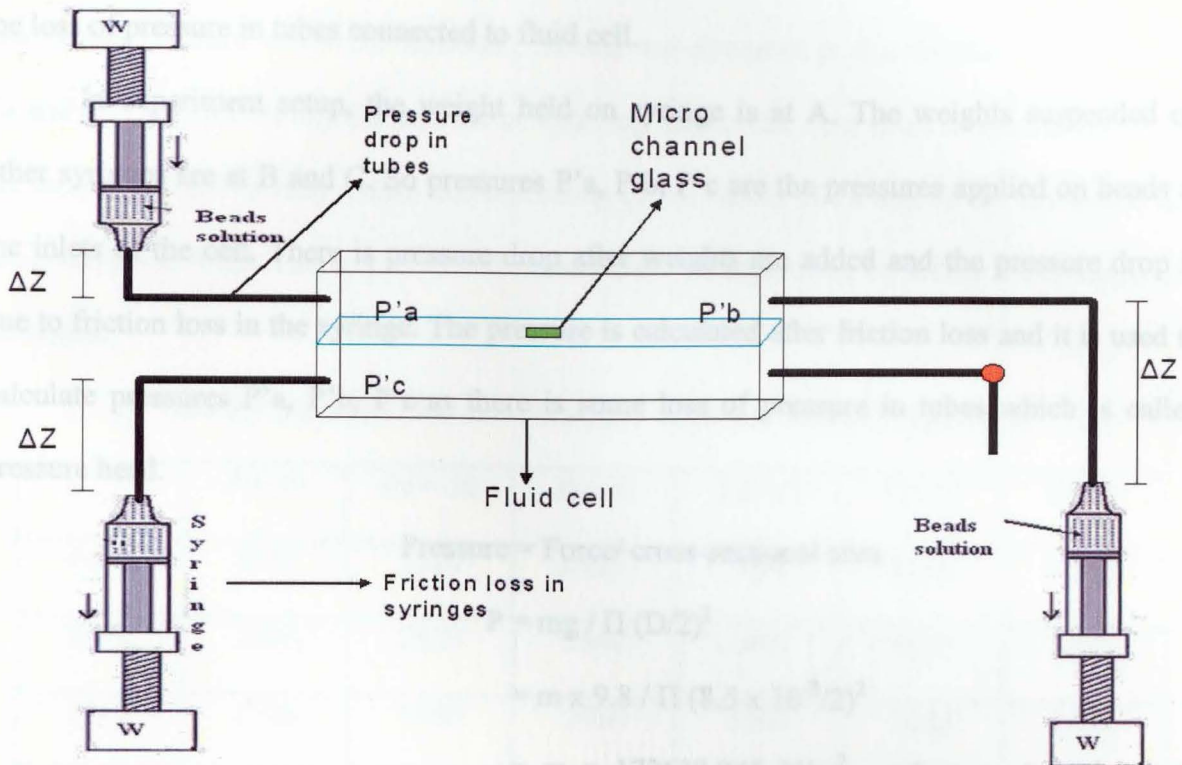


**Figure 4.2 Fluid Cell Experiment Setup with pressure applied**

The manipulation of beads can also be performed by applying pressure. Hence we tried applying pressures or varied pressure on all outlets without using syringe pumps. The setup is as shown in figure 4.2. The fluid cell outlets are connected to syringes through tubes. The syringes are held in a wooden block. Pressure is applied in all three syringes by putting weights on all syringes. The weights are kept on one syringe. The other weights are suspended on the other two syringes. So because of weights the pressure is created in the tubes connected to syringes. So the beads are under pressure and they are sent into fluid cell and are immobilized by varying the weights on the syringes. The pressure is calculated at different weights and the critical pressure in lower chamber is calculated for different pressures in the upper chamber.

Pressure in all the syringes can be calculated from its weight. There is loss of pressure applied on the beads. The pressure loss or pressure head is attributed to the friction loss in syringes and the loss of pressure in tubes connected to fluid cell.

In experiment setup, the weight held on syringe is at A. The weights suspended on other syringes are at B and C. So pressures P'a, P'b, P'c are the pressures applied on beads at the inlets of the cell. There is pressure drop after weights are added and the pressure drop is due to friction loss in the syringe. The pressure is calculated after friction loss and it is used to calculate pressures P'a, P'b, P'c as there is some loss of pressure in tubes which is called pressure head.

Pressure = Force/ cross-sectional area

$$P = mg / \Pi (D/2)^2$$

$$= m \times 9.8 / \Pi (8.5 \times 10^{-3}/2)^2$$

$$= m \times 172633.245 \text{ N/m}^2 \quad \text{where } m \text{ is the weight}$$

suspended or held on the syringes. So pressure after friction loss =  $m^* \times 172633.245 \text{ N/m}^2$ ;

Where  $m^* = (m - \text{friction loss weight})$  (units in grams)

The friction loss weight is different for different syringes. The friction loss weight for syringes at A and B is 60 g. The friction loss weight for syringe at C is 55 g. The pressures at A and B is maintained same by loading same weight. The weight at C is varied keeping weight at A and B same and pressures P'a, P'c are calculated. After the friction loss and the pressure loss in tube the final pressures P'a, P'c at the inlets of fluid cell are calculated and tabulated. The velocities corresponding to these P'a, P'c values are calculated and tabulated. The plot of Pa against Pc (P'a vs P'c) is plotted and is discussed in chapter5.

## 5 Results and Discussion

The resulting values obtained after the manipulation of beads is performed such as flow rate values, pressure values are tabulated, plotted and discussed in this chapter. The Values of  $F_a$  and  $F_c$  obtained during the process of applying automated flow rates to manipulate beads are tabulated. The velocity values corresponding to the values of  $F_a$  and  $F_c$  are calculated and are given in the table. The critical  $F_c$  values and their corresponding  $F_a$  values are obtained and tabulated.

**Velocity (speed) of the flow in upper chamber values (V)  $\mu\text{m}/\text{min}$**

	$F_a=10$	$F_a = 20$	$F_a=30$	$F_a=40$	$F_a=50$	$F_a=60$
$F_c=1$	2850	3540	4425	5900	8850	11800
$F_c=2$	2500	2500	3540	4425	8850	11800
$F_c=3$	1700	1960	2950	3540	7080	8850
$F_c=4$	1475	1600	2500	2950	7080	8850
$F_c=5$	1180	1360	2212	2520	5900	7080
$F_c=6$	983	1100	1960	2520	5900	7080
$F_c=7$	842	1040	1770	2212	4425	6436
$F_c=8$	632	983	1609	1960	3540	6400
$F_c=9$		885	1475	1770	3540	5900
$F_c=10$		842	1475	1609	2950	5440
$F_c=11$		708	1360	1475	2950	5057
$F_c=12$		632	1264	1360	2520	4720
$F_c=13$		610	1180	1360	2212	4425
$F_c=14$			1110	1260	2212	3930

Fc=15			1041	1260	1960	3520
Fc=16			983	1180	1863	3370
Fc=17			931	1110	1770	3218
Fc=18				1041	1685	2950
Fc=19				983	1539	2720
Fc=20				931	1475	2630
Fc=21				885	1416	2520
Fc=22					1360	2360
Fc=23					1264	2212
Fc=24					1212	2080
Fc=25					1180	1966
Fc=26					1141	1863
Fc=27						1770
Fc=28						1685
Fc=29						1610

**Table 5.1 Velocity of flow values corresponding to Fa and Fc values**

### Critical Fc values for Fa values

	Fc
Fa=10	8
Fa=20	14
Fa=30	17
Fa=40	22
Fa=50	26
Fa=60	29

**Table 5.2 Critical Fc values vs Fa values**

The Fa values and Fc values are plotted and also the critical Fc flow rate is appended. So we get a graph as shown. The area above straight line is not possible because we can't get flow rate of Fc more than that of Fa. The area under the straight line is area where we get clumping of beads because the flow rate of Fc increases and it is more than the critical flow rate of Fc. So after perfect array of beads in channels the beads start to clump on one another. The area under the critical flow rate curve is where there is less flow through channels and the beads don't experience much suction.

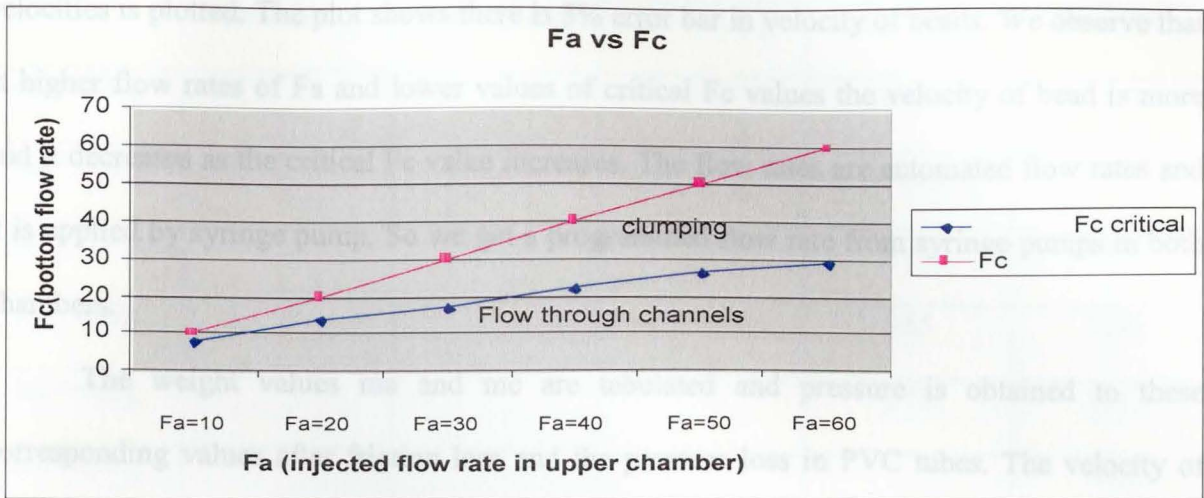


**Figure 5.1** Flow rate in upper chamber  $F_a$  vs Flow rate in lower chamber  $F_c$   
&  $F_a$  vs critical  $F_c$

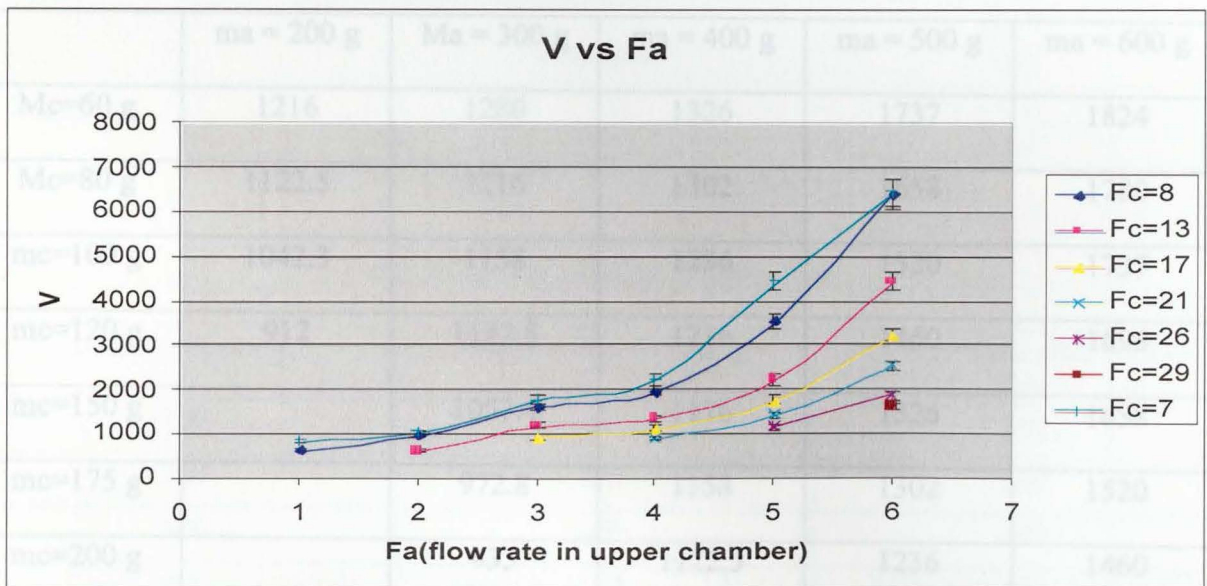


**Figure 5.2** Velocity of flow  $V$  vs Flow rate in upper chamber  $F_a$

The velocity of bead and the flow rate  $F_a$  is plotted at critical  $F_c$  values and is as shown where the velocity of beads values for different beads are considered and the range of



velocities is plotted. The plot shows there is 5% error bar in velocity of beads. We observe that at higher flow rates of  $F_a$  and lower values of critical  $F_c$  values the velocity of bead is more and it decreases as the critical  $F_c$  value increases. The flow rates are automated flow rates and it is applied by syringe pump. So we get a programmed flow rate from syringe pumps in both chambers.

The weight values  $m_a$  and  $m_c$  are tabulated and pressure is obtained to these corresponding values after friction loss and the pressure loss in PVC tubes. The velocity of beads is calculated at these different weights. There are different velocities for different corresponding  $m_a$  and  $m_c$  values. The pressures are calculated from weight values and the plots are discussed here.

#### Velocity (speed) of the beads in fluid cell (V) $\mu\text{m}/\text{min}$

	$m_a = 200 \text{ g}$	$M_a = 300 \text{ g}$	$m_a = 400 \text{ g}$	$m_a = 500 \text{ g}$	$m_a = 600 \text{ g}$
$M_c=60 \text{ g}$	1216	1280	1326	1737	1824
$M_c=80 \text{ g}$	1122.5	1216	1302	1658	1780
$m_c=100 \text{ g}$	1042.3	1158	1236	1520	1737
$m_c=120 \text{ g}$	912	1122.5	1216	1460	1696
$m_c=150 \text{ g}$		1057.4	1176	1326	1658
$m_c=175 \text{ g}$		972.8	1158	1302	1520
$m_c=200 \text{ g}$		935	1122.5	1236	1460
$m_c=225 \text{ g}$		890	1057.4	1216	1326
$M_c=250 \text{ g}$			1042.3	1176	1302
$m_c=275 \text{ g}$			1013.3	1140	1236
$m_c=300 \text{ g}$			972.8	1073	1216

	ma = 200 g	Ma = 300 g	ma = 400 g	ma = 500 g	ma = 600 g
mc=325 g				1042.3	1176
Mc=350 g				1013.3	1140
mc=375 g				995	1073
Mc=400g				985	1042
Mc=425g				978	1013
mc=450 g					995
mc=475 g					985
Mc=500g					978
Mc=525g					965

**Table 5.3 Velocity of bead flow in upper chamber to corresponding weights at A (ma) and**

**at C (mc)**

**ma or mb values after friction loss**

ma/mb values g	Friction loss weight g	ma/mb values after friction loss weight g
200	60	140
300	60	240
400	60	340
500	60	440
600	60	540

**Table 5.4 ma/mb values after friction loss weight in grams**

**mc values after friction loss**

mc values g	Friction loss weight g	mc values after friction loss g
60	55	5
80	55	25
100	55	45
120	55	65
150	55	95
175	55	120
200	55	145
225	55	170
250	55	195
275	55	220
300	55	245
325	55	270
350	55	295
375	55	320
400	55	345
425	55	370
450	55	395
475	55	420
500	55	445
525	55	470

**Table 5.5 mc values after friction loss weight in grams**

From these  $m_a$ ,  $m_b$ ,  $m_c$  values we calculate pressures after friction loss and these pressure values are used as the pressures at the tip of syringe i.e. at the starting of tube and we will find the pressures at the inlet of the tube. In general to find the pressure loss in a tube Bernoulli's equation is employed. So if we consider a tube which is as shown in figure 5.3 then changes in flow moving from point A to point B along a pipe is described by Bernoulli's equation

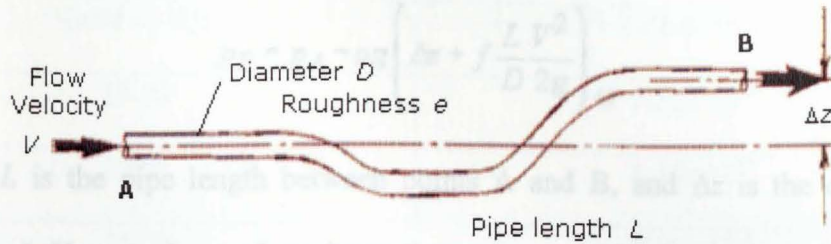


**Figure 5.3 Flow through bent tube from A to B and pressure loss in tube <sup>40</sup>**

Length of tubes(L)	$h = z(x) + \frac{p(x)}{\rho g} + \frac{V(x)^2}{2g}$ <sup>40</sup>	40 mm
Diameter of tube(D)		3.32 ~ 0.79375 mm

Where  $p$  is the pressure,  $V$  is the average fluid velocity,  $\rho$  is the fluid density,  $z$  is the pipe elevation above some datum, and  $g$  is the gravity acceleration constant.

Bernoulli's equation states that the total head  $h$  along a streamline remains constant. This means that velocity head can be converted into gravity head and/or pressure head, such that the total head  $h$  stays constant. No energy is lost in such a flow.

For real viscous fluids, mechanical energy is converted into heat (in the viscous boundary layer along the pipe walls) and is lost from the flow. Therefore Bernoulli's principle of conserved head (or energy) cannot be used to calculate flow parameters. The lost head by introducing another term (called *viscous head*) into Bernoulli's equation to get,

$$h = z + \frac{p}{\rho g} + \frac{V^2}{2g} + \int_{x_0}^x \frac{f}{D} \frac{V(\bar{x})^2}{2g} d\bar{x}$$
 <sup>40</sup>

Where  $D$  is the pipe diameter. As the flow moves down the pipe, viscous head slowly accumulates taking available head away from the pressure, gravity, and velocity heads. Still, the total head  $h$  (or energy) remains constant.

Pressure at point B,

$$P_B = P_A - \rho g \left( \Delta z + f \frac{L V^2}{D 2g} \right)_{40}$$

Where  $L$  is the pipe length between points A and B, and  $\Delta z$  is the change in pipe elevation ( $z_B - z_A$ ). Here we know the values of pressure  $p_A$ . The measured values of tube and height of tube at outlet of fluid cell from syringe pump are given.

Length of tubes(L)	40 mm
Diameter of tube(D)	1/32"= 0.79375 mm
Change in elevation $\Delta Z$	45 mm for syringes at B and C where weights are suspended
Change in elevation $\Delta Z$	60 mm for syringes at A where weights are held on syringe

Average fluid velocity in the tube ( $V_T$ ) is calculated by back calculation. As discussed flow rate  $Q = V$  (Velocity)  $\times$   $A$  (Area) where velocity  $V$  here is considered as velocity of beads. So  $Q$  can be calculated in the cell. Now flow rate in tube  $Q_T = V_T \times A_T$ . As flow rate values in tube and cell are considered of same value we can find  $V_T$ .

$$\text{Area of cell is } A = 1 \times 4.5 = 4.5 \text{ mm}^2$$

Therefore at different flow rates we get different values of velocity of beads in cell (Table 5.1 is considered). Now cross sectional Area of tube  $A_T = \pi D^2 / 4 = 0.5 \times 10^{-6} \text{ m}^2$ .

Therefore the average fluid velocity of tube  $V_T = Q_T / A_T \text{ m/s}$

( $\mu\text{l}/\text{min}$ ) $Q_T$	( $\text{m}/\text{s}$ ) $V_T$
15.93	$5.31 \times 10^{-4}$
19.91	$6.63 \times 10^{-4}$
26.55	$8.85 \times 10^{-4}$
39.82	$13.27 \times 10^{-4}$
53.10	$17.70 \times 10^{-4}$

**Table 5.6 Flow rate in tube  $Q_T$  vs Velocity of flow of beads in tube  $V_T$**

At different  $V_T$  values and different  $\Delta Z$  values we have different values of pressures at the inlets of fluid cell.

At  $V_T = 5.31 \times 10^{-4} \text{ m/s}$  and  $\Delta Z = 45 \text{ mm}$  (for B and C)

$$\begin{aligned}
 p_B &= p_A - \rho g \left( \Delta Z + f \frac{L V^2}{D 2g} \right)_{40} \\
 &= p_A - 1000 \times 9.8 [0.045 + f(0.04/0.00079375) \times (5.31 \times 10^{-4})^2 / \\
 &\quad (2 \times 9.8)]
 \end{aligned}$$

In order to calculate the pressures at inlets of fluid cell we need to find the values of  $f$  friction factor. The viscous head term is scaled by the pipe friction factor  $f$ . In general,  $f$  depends on the Reynolds Number  $R$  of the pipe flow, and the relative roughness  $e/D$  of the pipe wall,

$$f = f \left( R, \frac{e}{D} \right)_{40}$$

The roughness measure  $e$  is the average size of the bumps on the pipe wall. The relative roughness  $e/D$  is therefore the size of the bumps compared to the diameter of the pipe. Perfectly smooth pipes would have a roughness of zero.<sup>40</sup>

For laminar flow ( $R < 2000$  in pipes),  $f$  can be deduced analytically. The answer is,

$$f = \frac{64}{R} \quad 40$$

For turbulent flow ( $R > 3000$  in pipes),  $f$  is determined from experimental curve fits.

$$\frac{1}{\sqrt{f}} = -2 \cdot \log \left( \frac{e/D}{3.7} + \frac{2.51}{R\sqrt{f}} \right) \quad 40$$

The solutions to this equation plotted versus  $R$  make up the popular Moody Chart for pipe flow

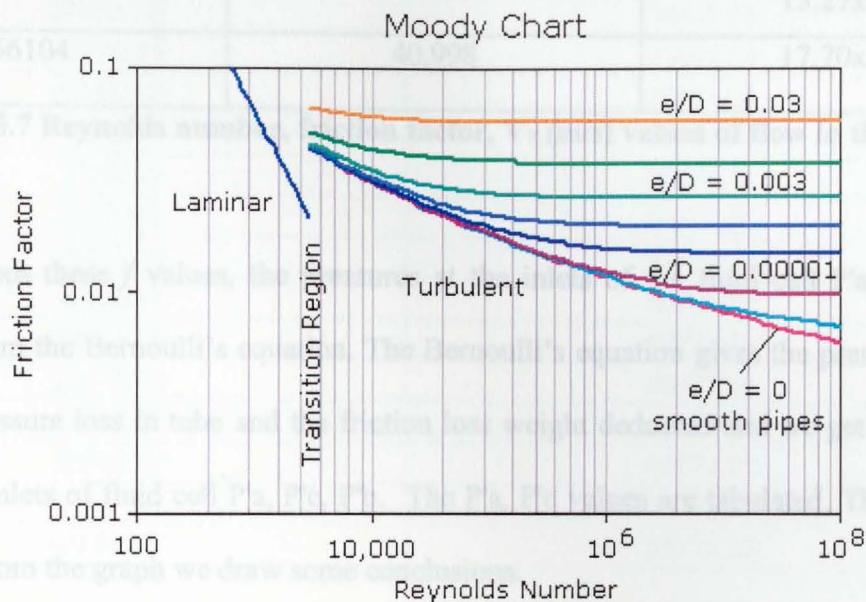


**Figure 5.4 Moody chart with Reynolds number vs Friction factor<sup>40</sup>**

The Reynolds Number for the flow can be computed. Then friction factor  $f$  is computed by direct substitution (if laminar) or by iteration using Newton-Raphson (if turbulent).

Reynolds number  $R = (\rho V_T D)/\mu$ ;  $\rho$  is the density;  $V_T$  is velocity of fluid in tube,  $D$  diameter of tube,  $\mu$  viscosity of fluid. For all  $V_T$  values the  $R$  values are calculated and their values are less than 10. So the flow is laminar in our experiment. The friction factor  $f$  is calculated by the formula given

$$f = 64 / R$$

So Reynolds number  $R$ , friction factor  $f$ , velocity of beads flow in tube  $V_T$  values are tabulated

Reynolds number $R$	Friction factor $f$	$(m/s)V_T$
0.4683	136.66	$5.31 \times 10^{-4}$
0.58472	109.45	$6.63 \times 10^{-4}$
0.78052	81.996	$8.85 \times 10^{-4}$
1.17033	54.6849	$13.27 \times 10^{-4}$
1.56104	40.998	$17.70 \times 10^{-4}$

**Table 5.7 Reynolds number, friction factor,  $V_T$  (m/s) values of flow in the tube**

So from these  $f$  values, the pressures at the inlets of the fluid cell P'a, P'c, P'b are calculated from the Bernoulli's equation. The Bernoulli's equation gives the pressure loss in a tube. The pressure loss in tube and the friction loss weight deducted and we get the values of pressures at inlets of fluid cell P'a, P'c, P'b. The P'a, P'c values are tabulated. The P'a, P'c are plotted and from the graph we draw some conclusions.



**P'a, P'c values**

P'c (N/m <sup>2</sup> )	P'a (N/m <sup>2</sup> )
254.57	23030.34
3628.76	23030.34
7002.95*	23030.34
10377.14^	23030.34
254.57	39901.28
3628.76	39901.28
7002.95	39901.28
10377.14	39901.28
15438.42	39901.28
19656.15*	39901.28
23873.89	39901.28
28091.62^	39901.28
254.57	56772.28
3628.76	56772.28
7002.95	56772.28
10377.14	56772.28
15438.42	56772.28
19656.15	56772.28
23873.89	56772.28
28091.62	56772.28
32309.36*	56772.28
36527.09	56772.28
40744.83^	56772.28

Table 5.3 P'a, P'c values with critical arraying P'c\* and critical clamping P'c^ values to corresponding P'a values

Contd.

$P'_c$ (N/m <sup>2</sup> )	$P'_a$ (N/m <sup>2</sup> )
254.57	73643.16
3628.76	73643.16
7002.95	73643.16
10377.14	73643.16
15438.42	73643.16
19656.15	73643.16
23873.89	73643.16
28091.62	73643.16
32309.36	73643.16
36527.09	73643.16
40744.83	73643.16
44962.56	73643.16
53398.03*	73643.16
57615.77	73643.16
61833.5	73643.16
66051.24^	73643.16
254.57	91044.1
3628.76	91044.1
7002.95	91044.1
10377.14	91044.1
15438.42	91044.1
19656.15	91044.1
23873.89	91044.1
28091.62	91044.1
32309.36	91044.1
36527.09	91044.1
40744.83	91044.1
44962.56	91044.1
53398.03	91044.1
57615.77	91044.1
61833.5*	91044.1
66051.24	91044.1
70268.97	91044.1
74486.71	91044.1
78704.44^	91044.1

**Table 5.8  $P'_a$ ,  $P'_c$  values with critical arraying  $P'_c^*$  and critical clumping  $P'_c^{\wedge}$  values to corresponding  $P'_a$  values**

The beads movement is recorded and analyzed by optical microscopy and video recording. The optical micrographs are as shown when suction is applied by applying flow rate with certain pressure. The beads are forming an array when a critical flow rate is reached.

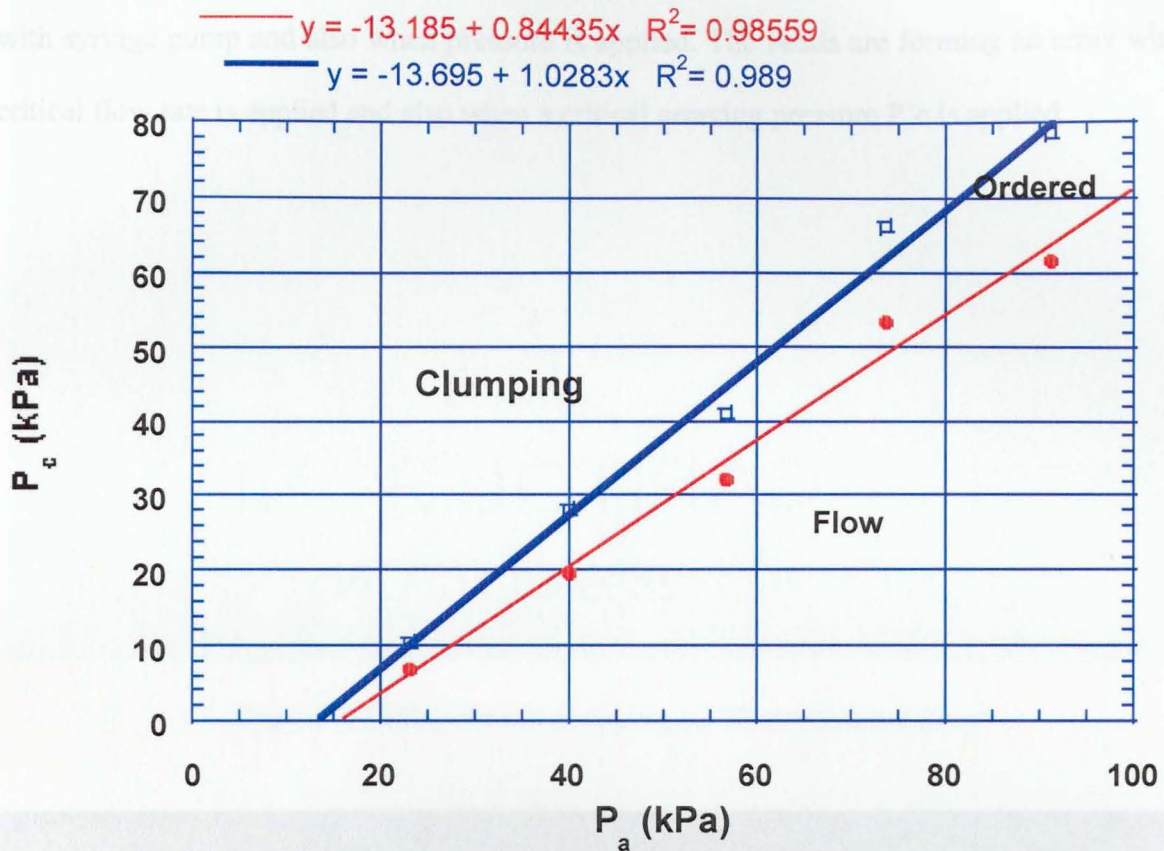


**Figure 5.5  $P_a$  vs  $P_c$  values**

The graph between  $P'_a$  and  $P'_c$  shows that initially there is flow of beads when the load at C is less. After gradual increase in load at C suction increases and the flow of beads slows down forming an array. It reaches a phase where there is an ordered form of beads. On increasing the load further at C the suction is increased considerably high enough that the beads start to clump and the clumping phase can be seen in the graph. So the manipulation of these beads is best suited when the suction is applied at a point where ordering of beads take place. So the pressures  $P'_a$  and  $P'_c$  at ordered phase are the critical pressures for easy manipulation of the beads.

The beads movement is assessed and analyzed by optical microscopy and video is recorded. The optical micrographs are as shown when suction is applied by applying flow rate with syringe pump and also when pressure is applied. The beads are forming an array when a critical flow rate is applied and also when a critical arraying pressure  $P^*c$  is applied.

Figure 5.7 Microbeads arraying on Microchannel glass

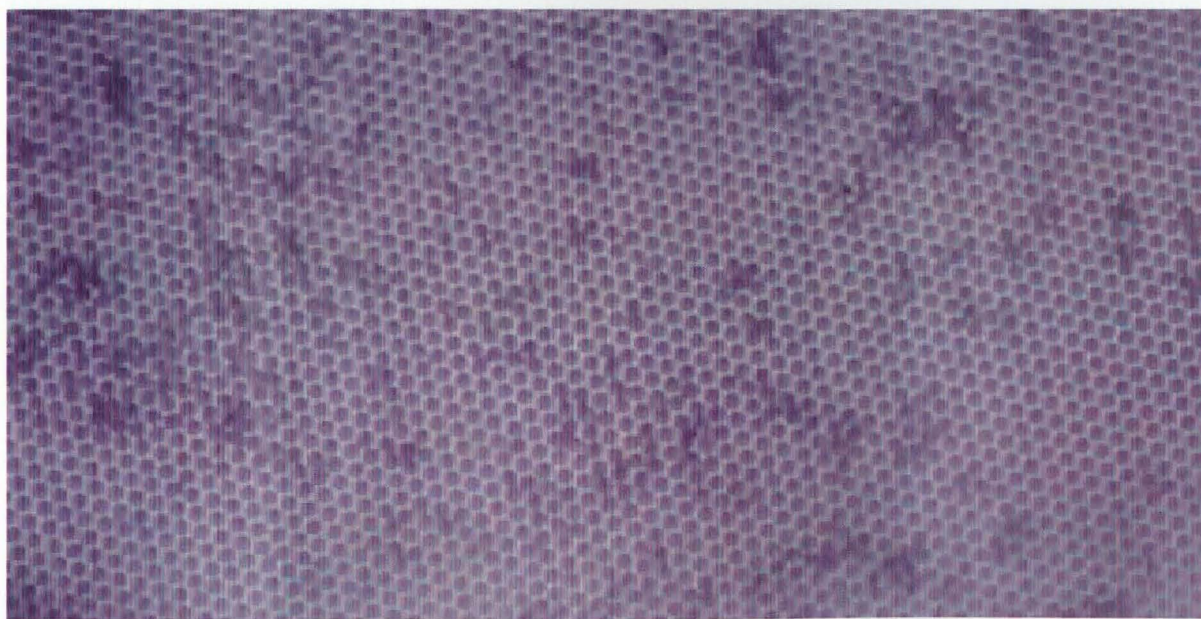


Figure 5.6 Microbeads arraying on Microchannel glass



**Figure 5.7 Microbeads arraying on Microchannel glass**



**Figure 5.8 Microbeads arraying on Microchannel glass**

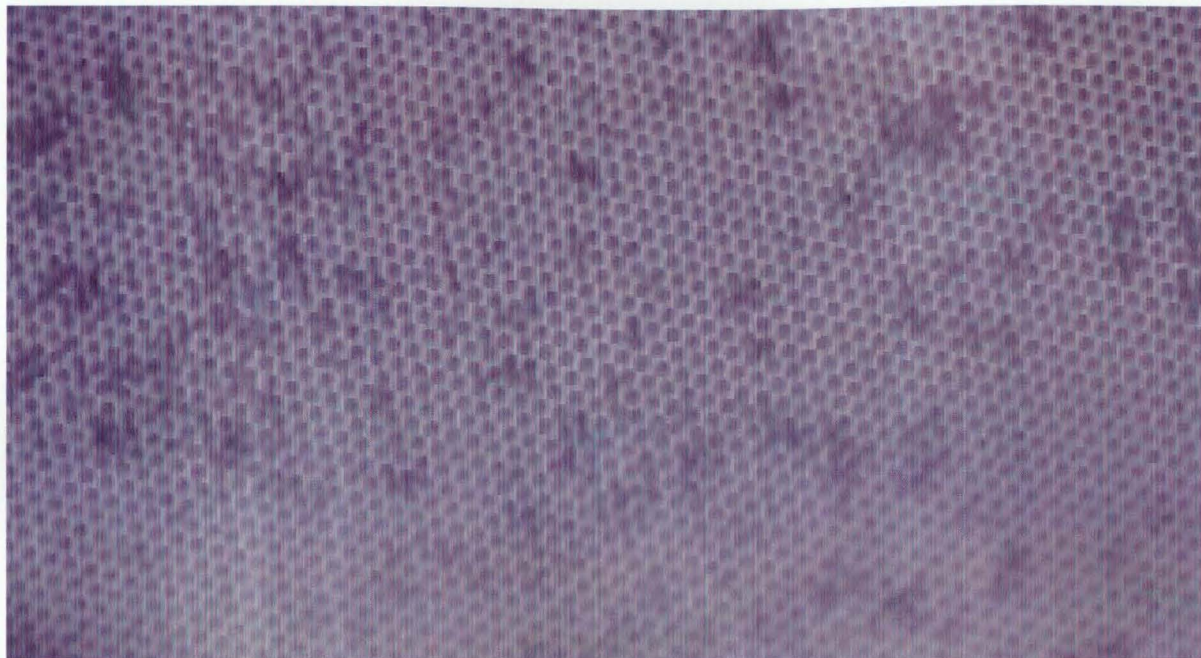


**Figure 5.8 Microbeads arraying on Microchannel glass**

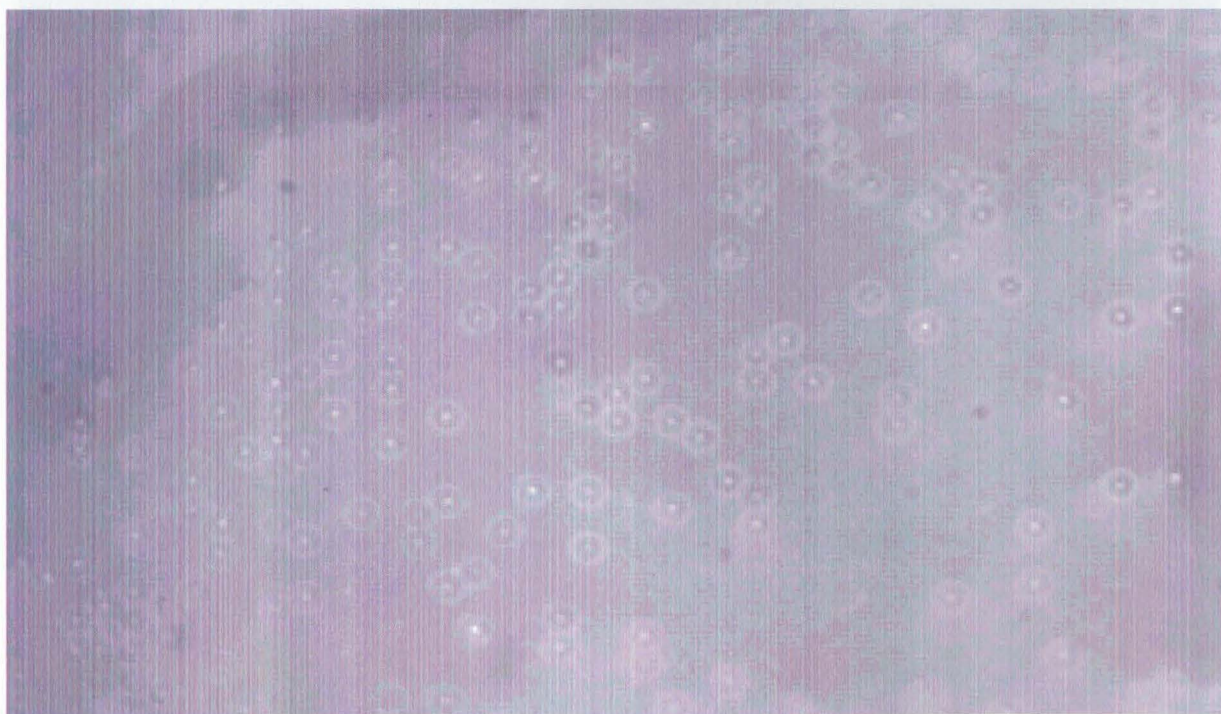


**Figure 5.9 Microbeads arraying on Microchannel glass**

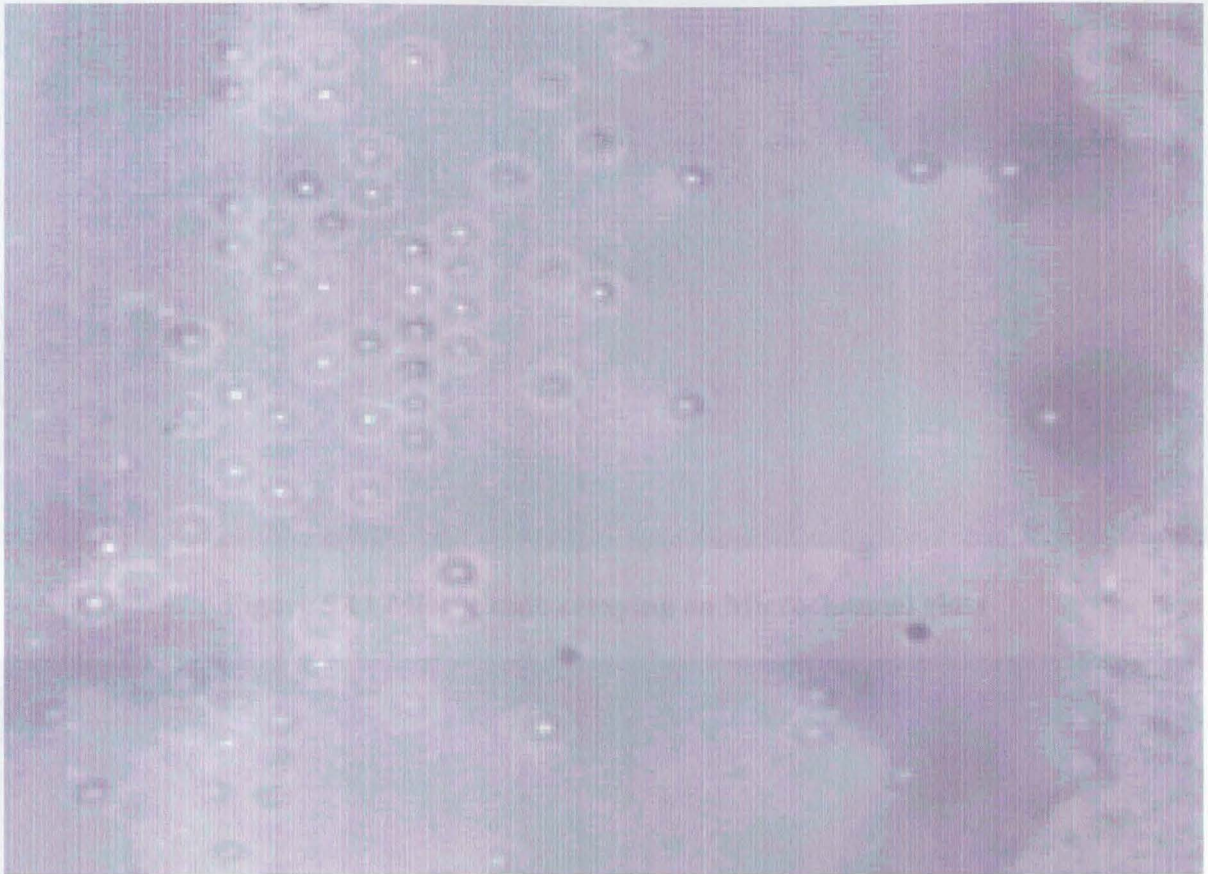


**Figure 5.10 Microbeads arraying on Microchannel glass**

*Figure 5.12 Microbeads arraying on Microchannel glass*

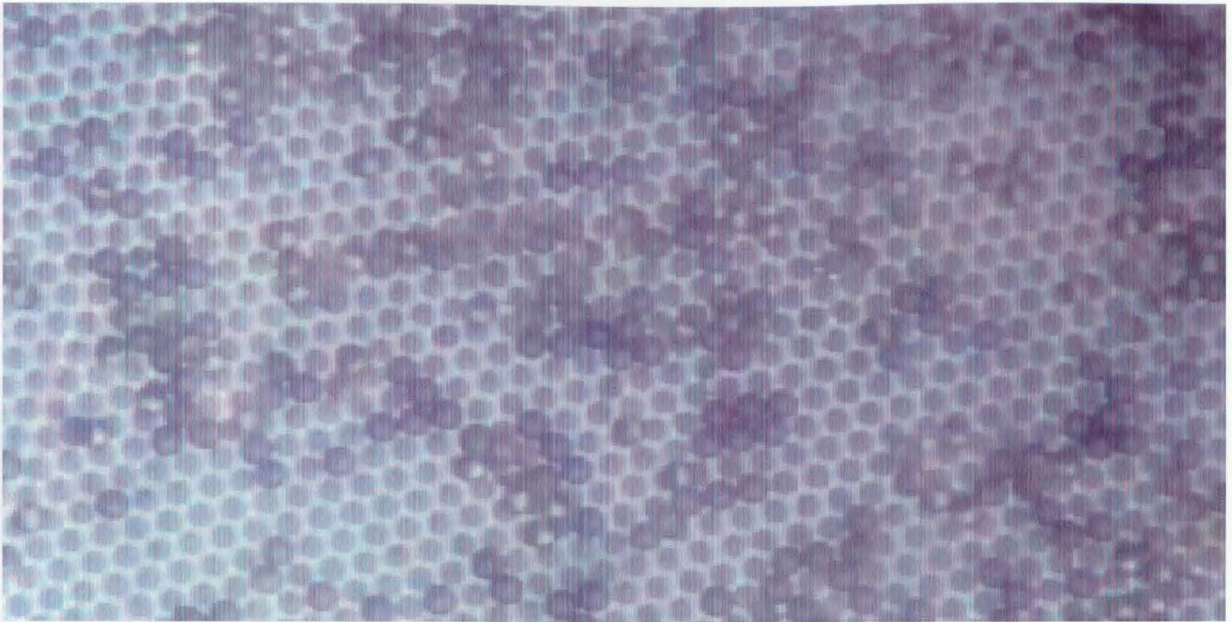


**Figure 5.11 Microbeads arraying on Microchannel glass**



**Figure 5.12 Microbeads arraying on Microchannel glass**

*Figure 5.14 Clumping of microbeads on microchannel glass*



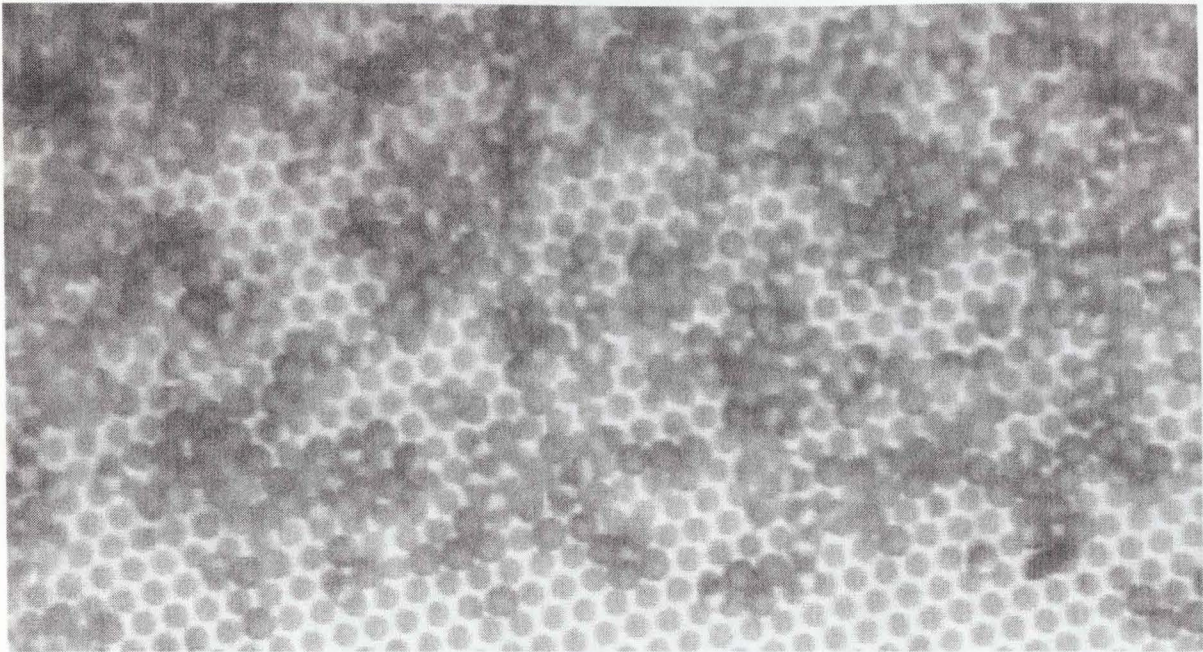


**Figure 5.13 Microbeads arraying on Microchannel glass**

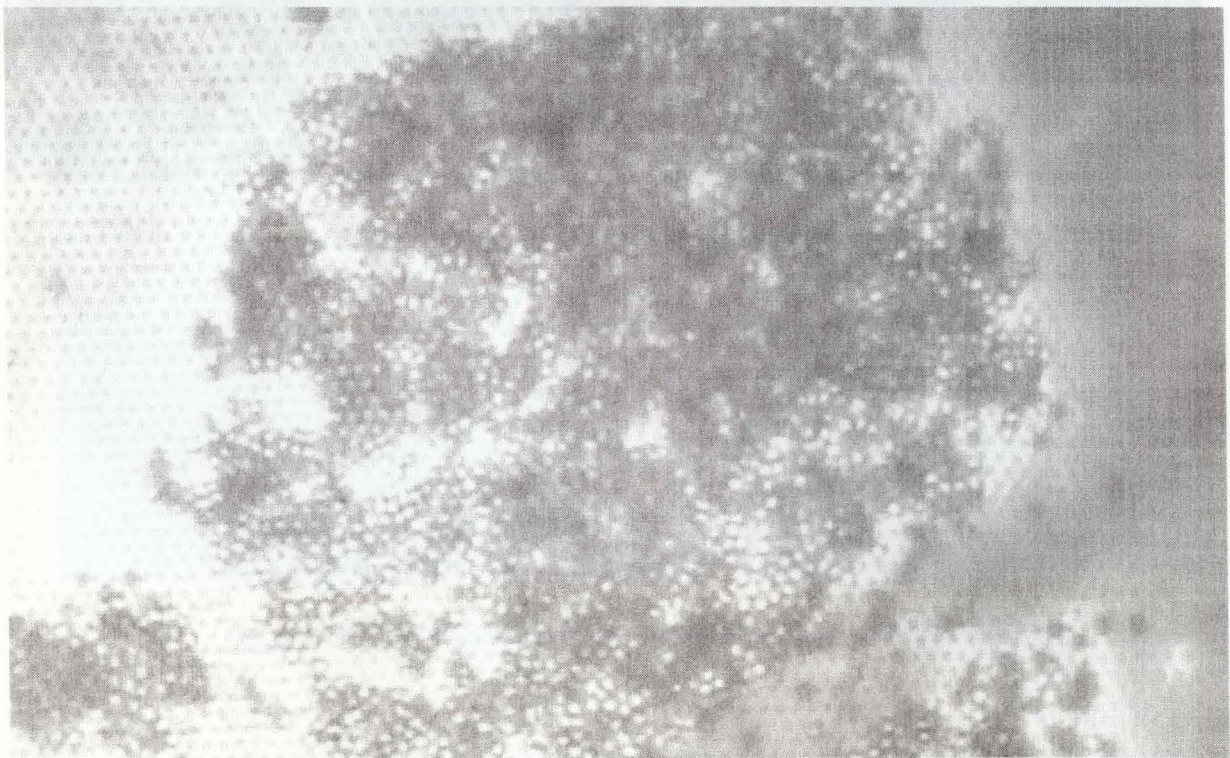


**Figure 5.14 Clumping of microbeads on microchannel glass**

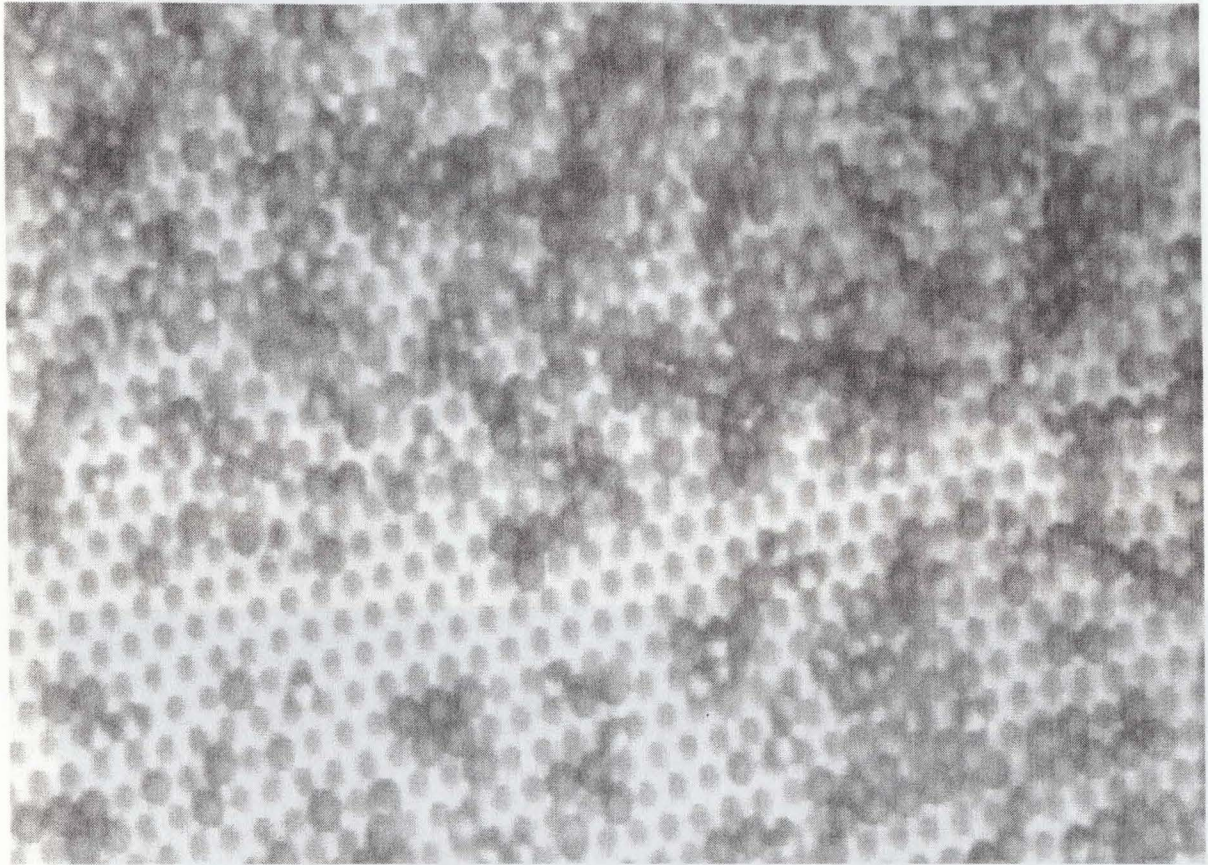


**Figure 5.15 Microbeads arraying on Microchannel glass**

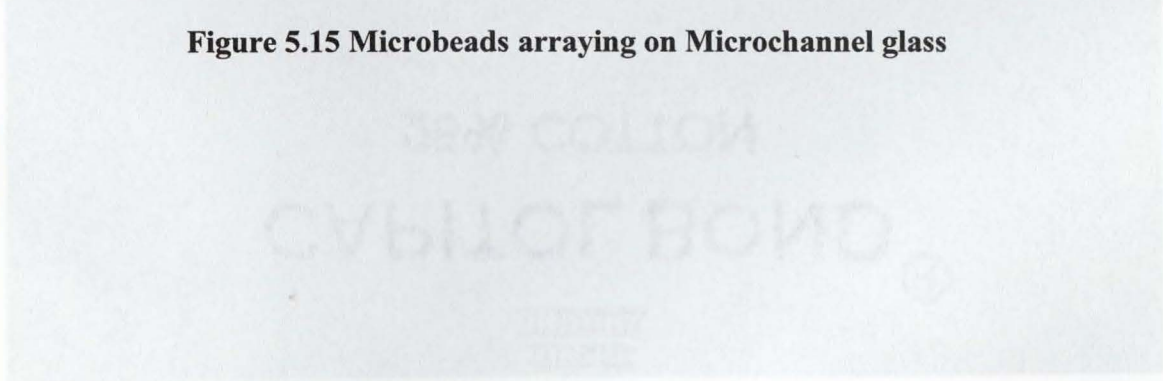


**Figure 5.17 Clumping of microbeads on microchannel glass**

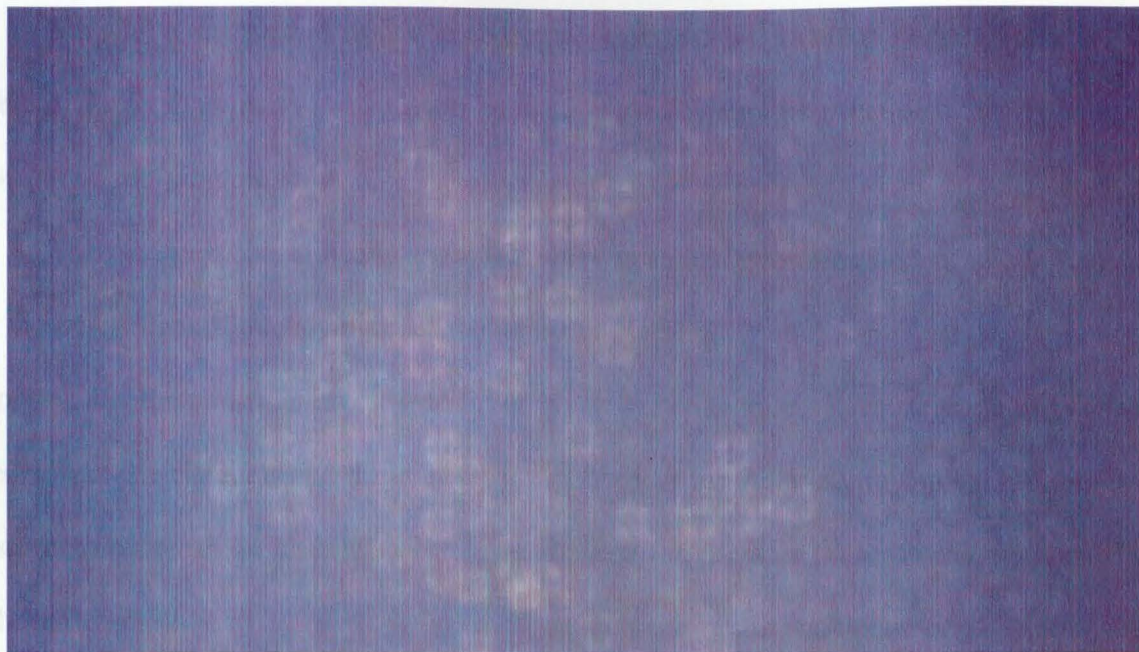


**Figure 5.16 Microbeads arraying on Microchannel glass**

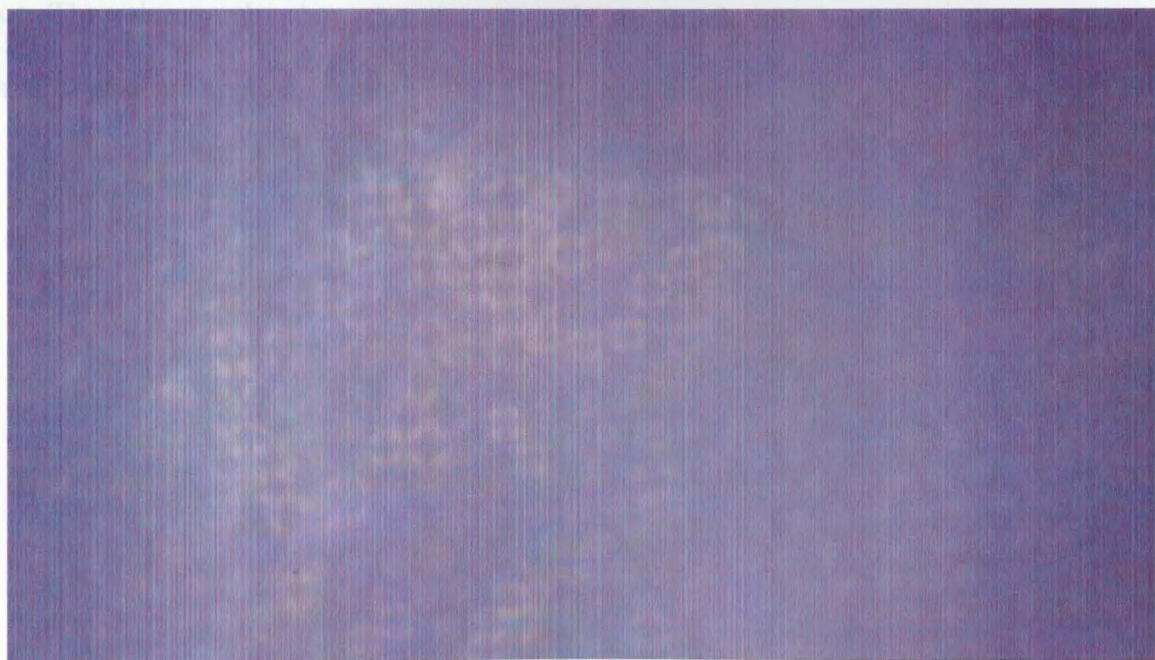


**Figure 5.17 Clumping of microbeads on microchannel glass**

The video recorded is copied to a compact disc and is submitted along with thesis. The different videos show that the beads can be manipulated by applying suction either by applying flow rate or applying pressure.

The manipulation of beads show that there is an array forming on microchannel glass. But the percentage of occupying channels is about 30-50% of the channel glass when pressure is applied and the reason is investigated. The occupancy rate is less because some of the beads are struck in the channels and these beads act as barriers for the pressure applied. So the beads would not occupy those channels. When we increase the pressure there is critical point where all beads form an array. After that critical pressure the beads start clumping. Due to beads struck in the channels the clumping of beads start before the channels are completely filled. So this is the reason why after 30-50% occupancy of channels with beads clumping of beads takes place. The micrographs show that the channels are struck with beads and the beads act as barrier to pressure applied.

Figure 3.18 Microbeads struck to channels of microchannel glass

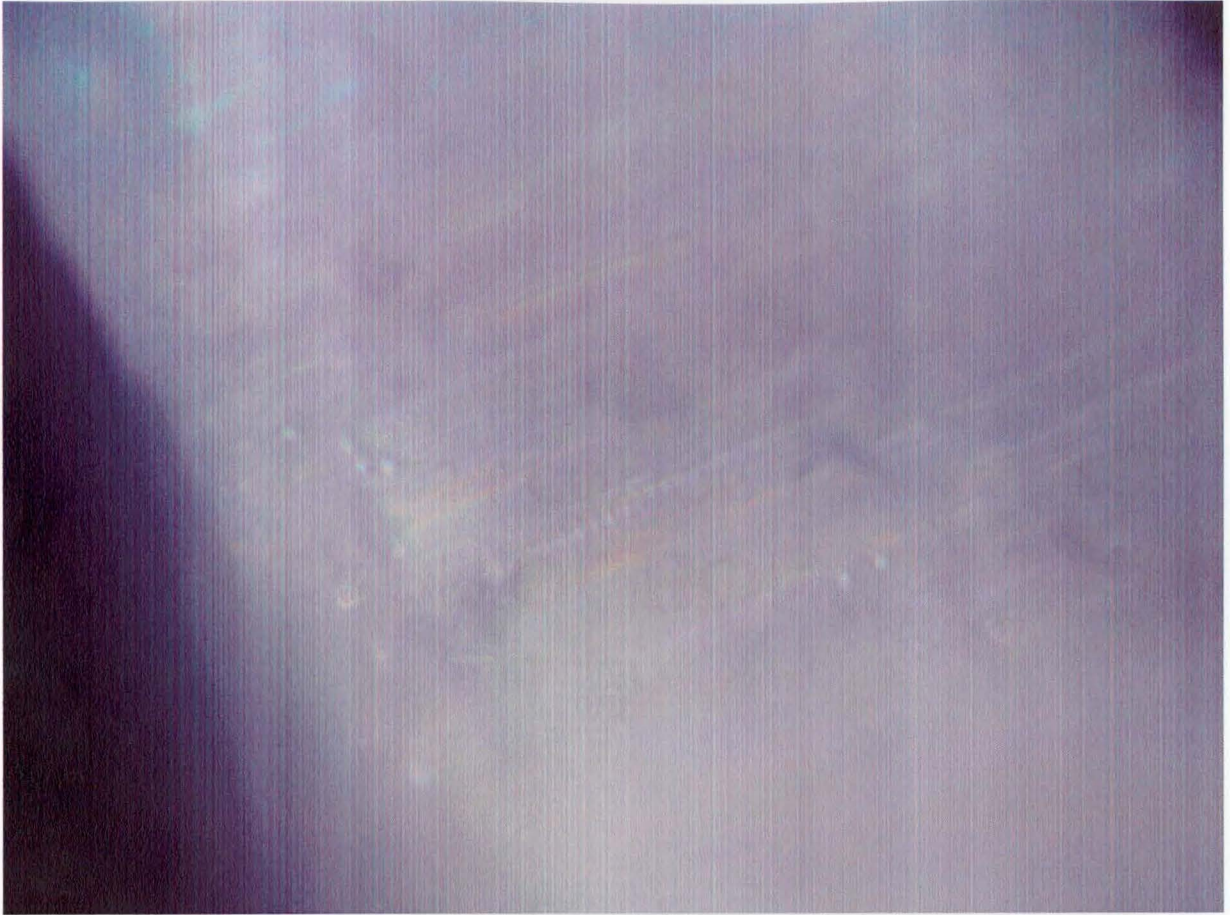


**Figure 5.18 Microbeads struck in channels of microchannel glass**

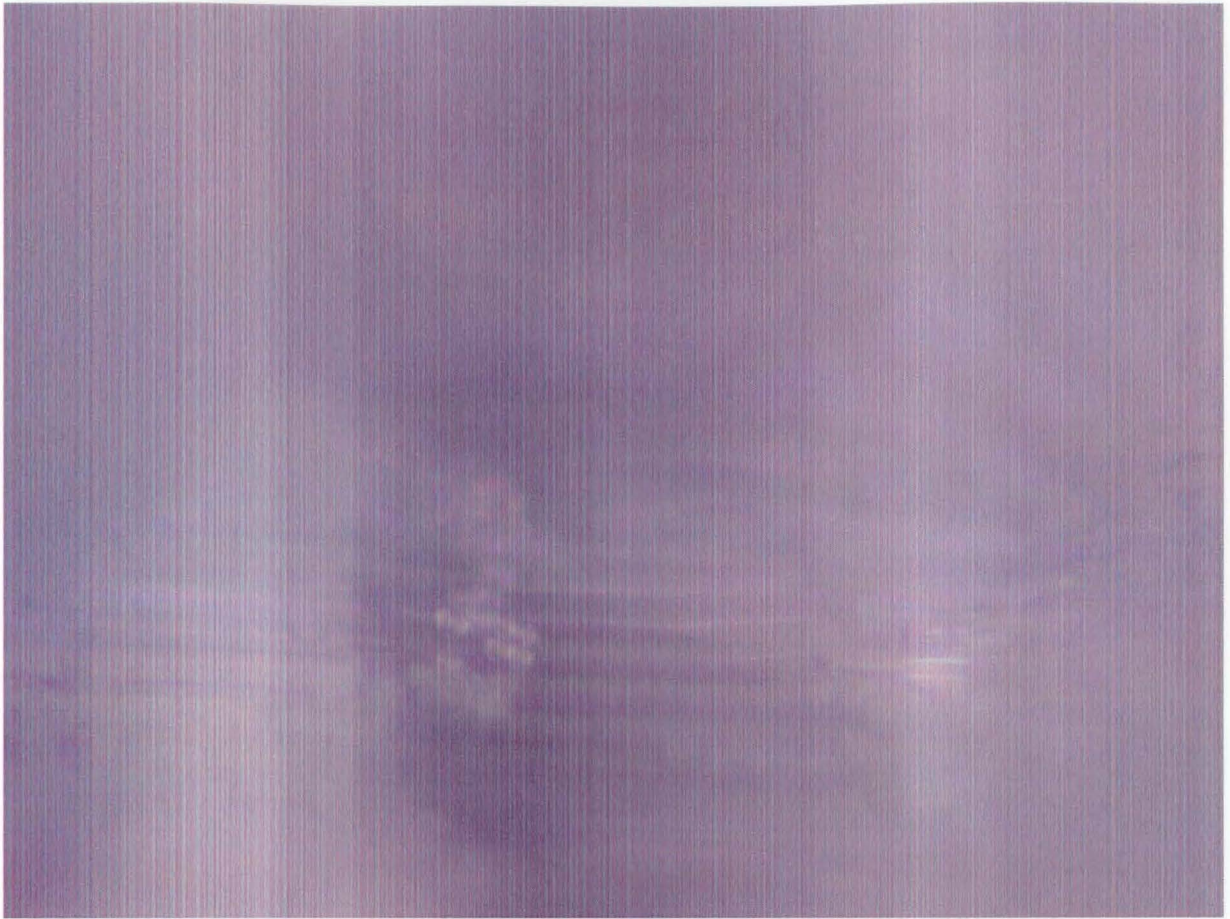


**Figure 5.19 Microbeads stuck in channels of microchannel glass**

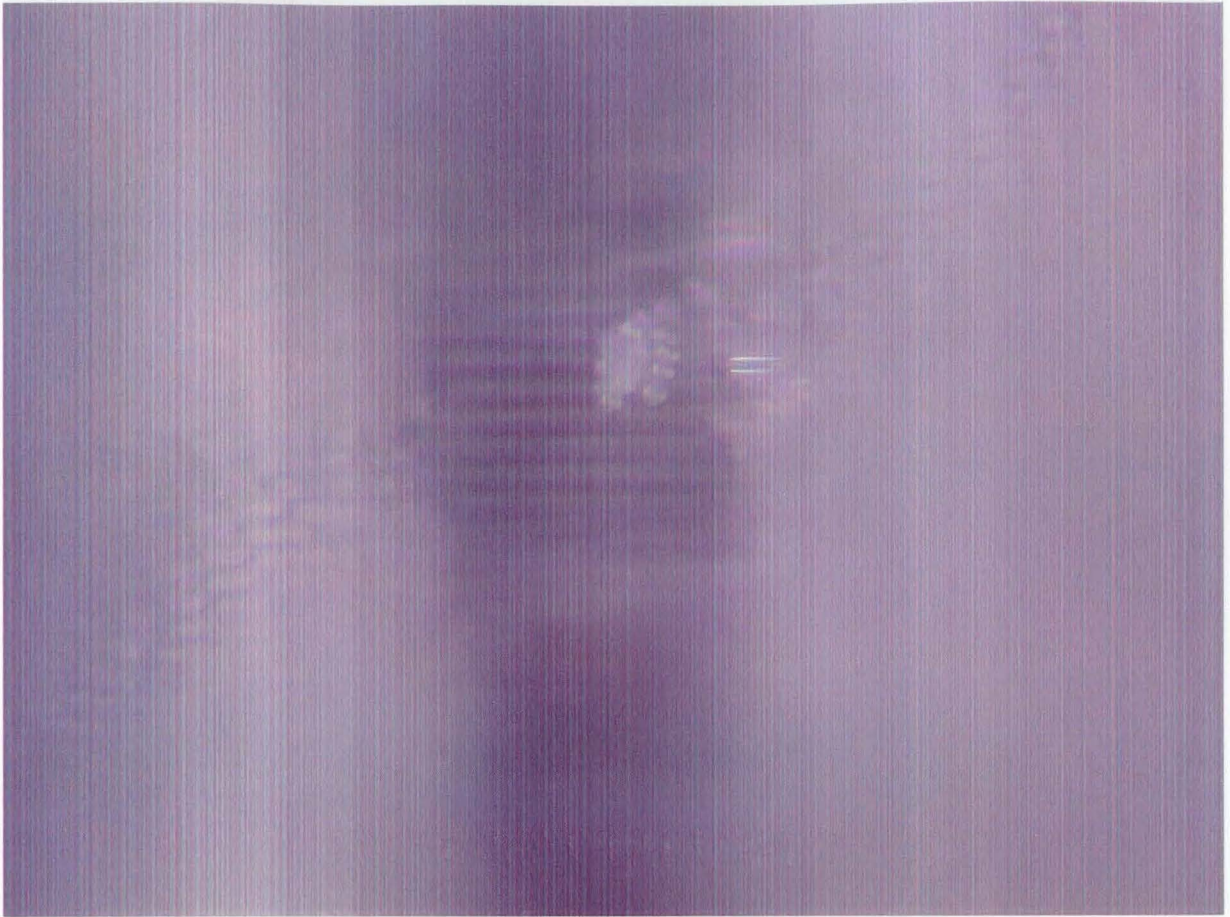


**Figure 5.20 Microbeads stuck in channels of microchannel glass**

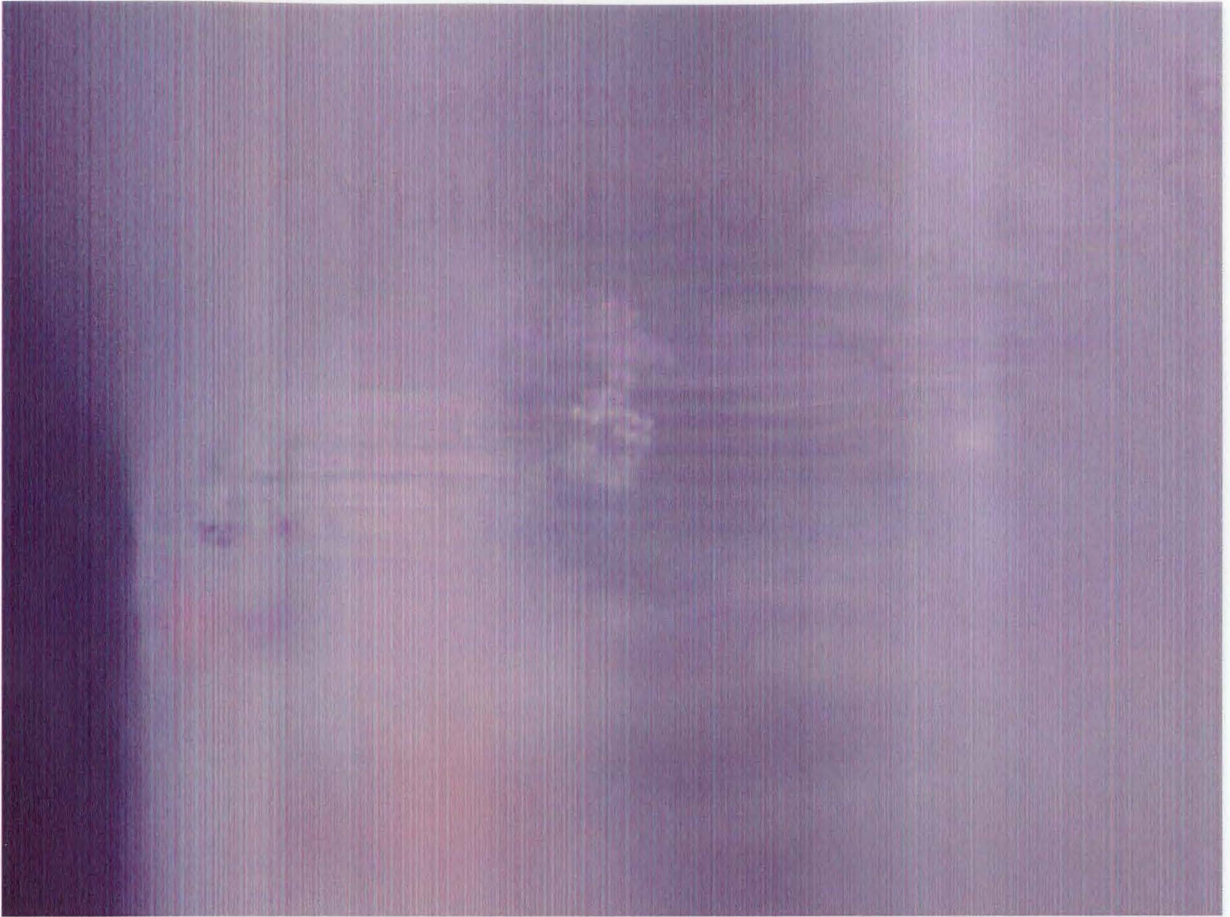


**Figure 5.21 Microbeads stuck in channels of microchannel glass**



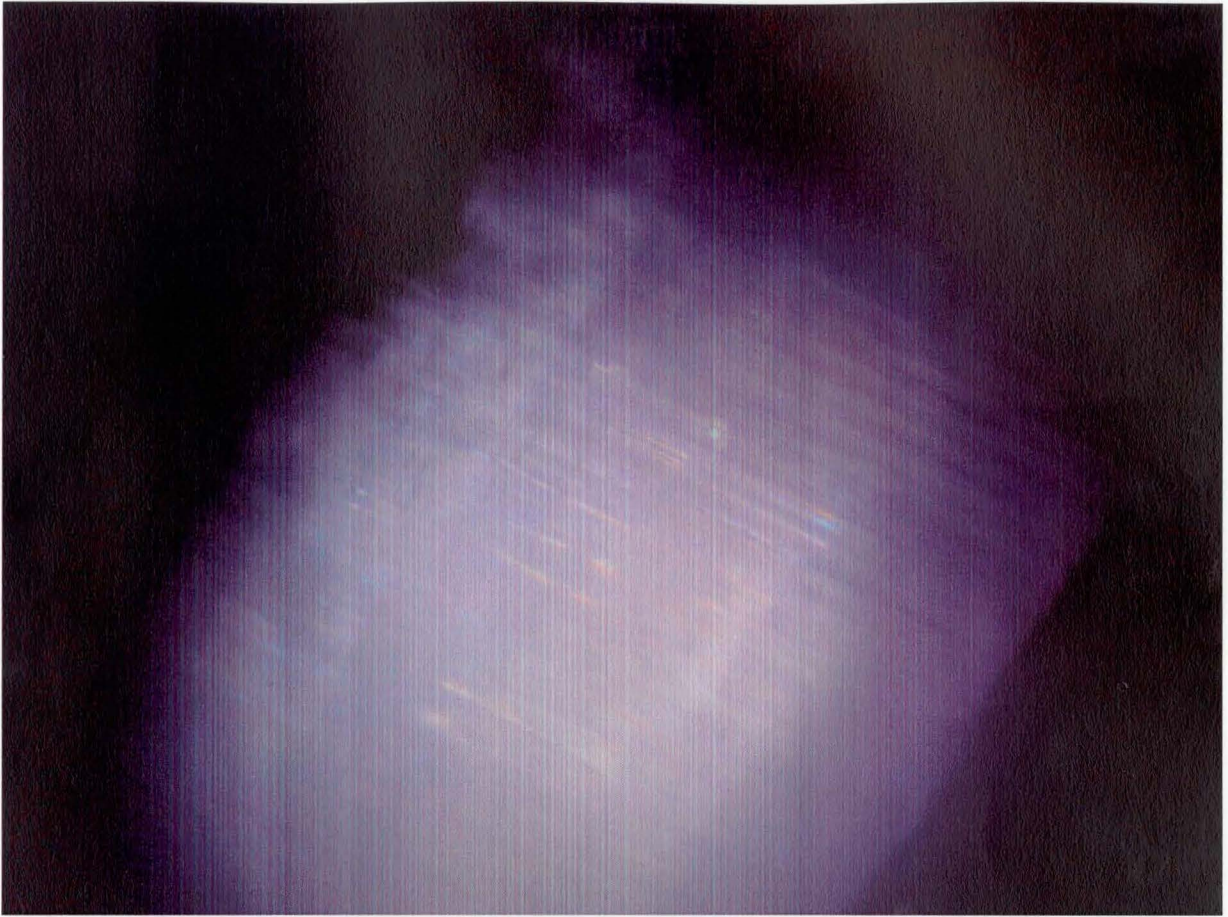


**Figure 5.22 Microbeads struck in channels of microchannel glass**

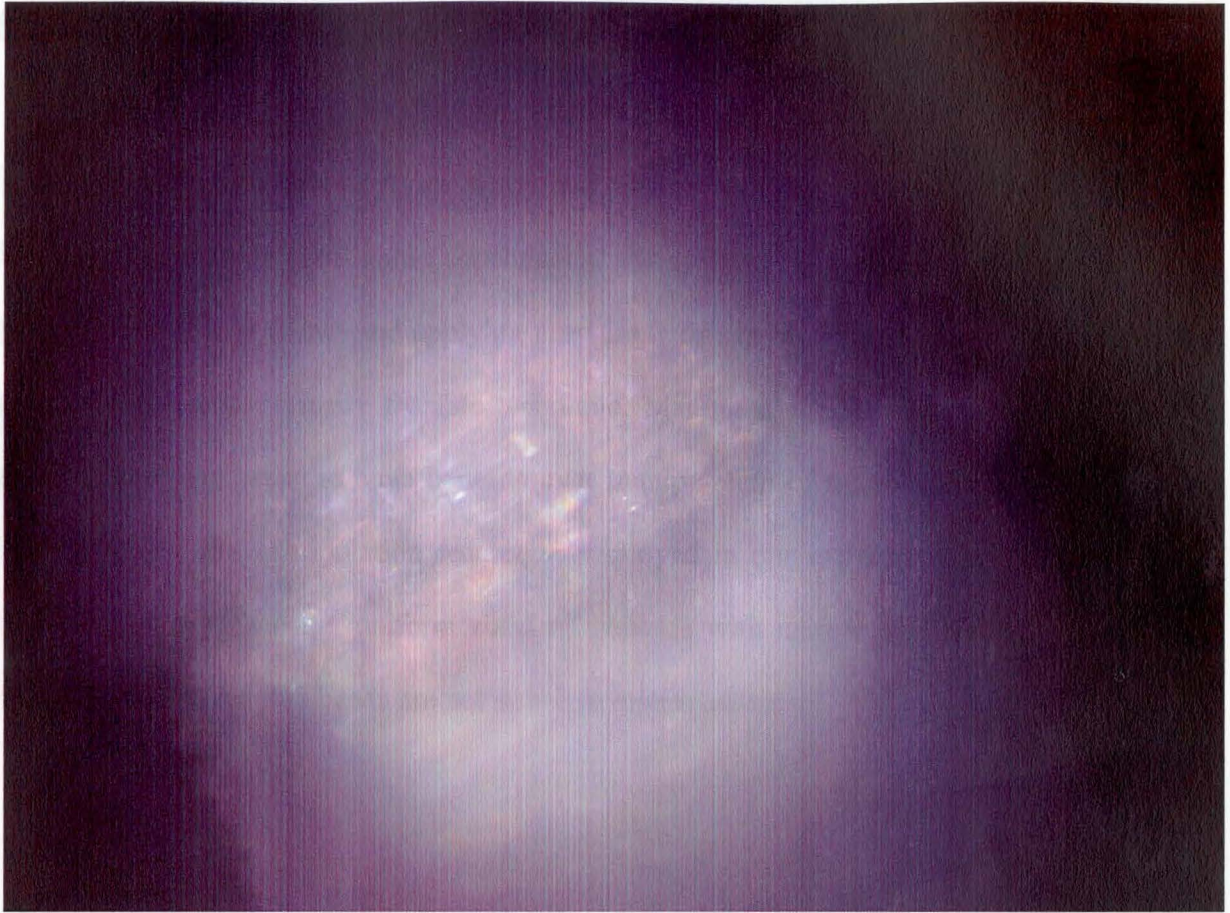


**Figure 5.23 Microbeads stuck in channels of microchannel glass**

## 6 Conclusions and Future work

The Manipulation of microbeads on a microchannel glass is done by applying variable flow rates with the help of syringe pump and also by applying pressure with weights. From these experiments we drew some conclusions. Manipulation of microbeads on microchannel glass by applying flow rate and applying pressure is one of the best techniques employed and moreover it is economically feasible technique. Manipulating microbeads on microchannel glass by applying pressure have benefits over manipulation of microbeads by applying flow rate. In future, the manipulation technique employed in our experiment can be used in an effective way by choosing uniform sized microbeads with narrow size distribution and also care should be taken that beads are not struck in microchannels.

applications", *Microfluid Nanofluid*, vol. 1, pp. 22-51, 2004

\* Jian-Guo Guan, Yu Qiang-Miao, Qing-Xu Zhang "Impedimetric Biosensors", *Journal of Bioscience and Bioengineering*, no.4, vol. 97, pp. 219-226, 2004

<http://www.fal.gov.it/~/media/ital>

\* Elizabeth Verpoorte "Beads and drops: new concepts for analysis" *Lab Chip*, vol. 3, pp. 60-63, 2003

\* Mingyong Han, Xiaohu Guo, Jack E. Sa, Shengqiang Nie "Quantum-dot-tagged microbeads for multiplexed optical encoding of biomolecules", *Nature biotechnology*, vol. 19, pp. 631-635, 2001

\* TechNote # 301 Becton Dickinson Inc. "Flow cytometry applications"

\* Benjamin D.Mattews, David A.LaVita, Darryl R.Overby, John Karavitis, and Donald E. Ingber "Electromagnetic needles with induction pole tip radii for nanomanipulation of biomolecules and living cells", *Applied Physics letters*, no.14, vol. 85, pp. 2964-2970, 2004

## REFERENCES

- <sup>1</sup> Elizabeth Mirowski, John Moreland, and Stephen E. Russek, *Electronics and Electrical Engineering Laboratory, National Institute of Standards and Technology*, Michael J. Donahue *Information Technology Laboratory, National Institute of Standards and Technology* “Integrated microfluidic isolation platform for magnetic particle manipulation in biological systems”, *Applied Physics letters*, no.10, vol. 84, pp. 1786-1788, 2004
- <sup>2</sup> Zong-Ping Luo, Yu-Long Sun, and Kai-Nan An *Biomechanics Laboratory, Mayo Clinic, Rochester, Minnesota* “An optical spin micromotor”, *Applied Physics letters*, no.13, vol. 76, pp.1779-1781, 2000
- <sup>3</sup> Martin A.M.Gijs “Magnetic bead handling on-chip: new opportunities for analytical applications”, *Microfluid Nanofluid*, vol. 1, pp. 22-40, 2004
- <sup>4</sup> Jian-Guo Guan, Yu Qing-Miao, Qing-Jie Zhang “Impedimetric Biosensors”, *Journal of Bioscience and Bioengineering*, no.4, vol. 97, pp. 219-226, 2004
- <sup>5</sup> <http://www.llnl.gov/str/Miles.html>
- <sup>6</sup> Elisabeth Verpoorte “Beads and chips: new recipes for analysis” *Lab Chip*, vol. 3, pp. 60-68, 2003
- <sup>7</sup> Mingyong Han, Xiaohu Gao, Jack Z. Su, Shuming Nie “Quantum-dot-tagged microbeads for multiplexed optical encoding of biomolecules”, *Nature biotechnology*, vol. 19, pp. 631-635, 2001
- <sup>8</sup> TechNote # 301 Bangs Laboratories Inc. “Immunological applications”
- <sup>9</sup> Benjamin D.Matthews, David A.LaVan, Darryl R.Overby, John Karavitis, and Donald E. Ingber “Electromagnetic needles with submicron pole tip radii for nanomanipulation of biomolecules and living cells”, *Applied Physics letters*, no.14, vol. 85, pp. 2968-2970, 2004

<sup>10</sup> Mathieu Allard, Edward H. Sargent, Patrick C. Lewis, and Eugenia Kumacheva “Colloidal Crystals grown on Patterned surfaces”.

<sup>11</sup> Helene Andersson Microsystem Technology Department of Signals, Sensors and Systems Royal Institute of technology “Microfluidic devices for Biotechnology and organic chemical applications”.

<sup>12</sup> <http://www.stanford.edu/group/blocklab/Optical%20Tweezers%20Introduction.htm>

<sup>13</sup> Applied Physics B “Laser and optics”

Department of Physics, Faculty of Science, National University of Singapore

Centre for Ion Beam Applications, Department of Physics, National University of Singapore

Department of Mechanical Engineering, Faculty of Engineering, National University of

Singapore, “Multiple-spot optical tweezers created with micro lens arrays fabricated by proton beam writing”, Applied Physics B-Laser and Optics, vol. 78, pp. 705-709, 2004

<sup>14</sup> Fumihito Arai, Akihiko Ichikawa, Hisataka Maruyama, Kouhei Motoo, and Toshio Fukuda “Manipulation of single cell for separation and Investigation”, International Journal of Control, Automation, and Systems, no.2, vol. 2, pp. 135-143, 2004

<sup>15</sup> <http://www.igmors.u-psud.fr/duguet/webEAN/fig.gif/Diapositive1.jpg>

<sup>16</sup> Benjamin D. Matthews, David A. LaVan, Darryl R. Overby, John Karavitis, and Donald E. Ingber “Electromagnetic needles with submicron pole tip radii for nanomanipulation of biomolecules and living cells”, Applied Physics letters, no.14, vol. 85, pp. 2968-2970, 2004

<sup>17</sup> G. Medoro, N. Maresi, Silicon Biosystems s.r.l., A. Leonardi, L. Altomare, M. Tartagni, R. Guerrieri, ARCES, University of Bologna “A lab-on-a-chip For Cell Detection and Manipulation”

- <sup>18</sup> N.Manaresi, G.Medoro, L.Altomare, M.Tartagni and R.Guerrieri *University of Bologna*  
“Microelectronics meets Biology: Challenges and Opportunities for functional integration in  
Lab-on-chip” <http://www.nano-optics.ethz.ch/research/spon-emiss.htm>
- <sup>19</sup> <http://www.nano-optics.ethz.ch/research/spon-emiss.htm>
- <sup>20</sup> <http://www.cs.unc.edu/Research/nano/cisimm/3d/index.html>
- <sup>21</sup> Tobias Lilliehorn “Piezoactuators for Microfluidics Towards Dynamic Arraying”, printed in  
Sweden by Fyris-Tryck AB, Uppsala, 2003
- <sup>22</sup> Muhammet Kursad Araz *Applied and Engineering Physics*, Chung-Hoon Lee *School of  
Electrical and Computer Engineering*, Amit Lal *Sonic MEMS Laboratory, Cornell University*  
“Ultrasonic Separation in Microfluidic Capillaries”, IEEE Ultrasonic symposium, pp. 1066-  
1069, 2003
- <sup>23</sup> [http://www.ncbi.nlm.nih.gov/entrez/query.fcgi?cmd=Retrieve&db=PubMed&list\\_uids=7765  
041&dopt=Abstract](http://www.ncbi.nlm.nih.gov/entrez/query.fcgi?cmd=Retrieve&db=PubMed&list_uids=7765041&dopt=Abstract)
- <sup>24</sup> Elizabeth Mirowski, John Moreland, Arthur Zhang and Stephen E. Russek, *Electronics and  
Electrical Engineering Laboratory, National Institute of Standards and Technology*, Michael  
J. Donahue *Information Technology Laboratory, National Institute of Standards and  
Technology* “Manipulation and sorting of magnetic particles by a magnetic force microscope  
on a microfluidic magnetic trap platform”, *Applied Physics letters*, vol. 86, pp. 243901-1 –  
243901-2, 2005
- <sup>25</sup> P.Jordan, H. Clare, L.Flendrig, J.Leach, J.Cooper, M.Padgett “Permanent 3D microstructures  
in a polymeric host created using holographic optical tweezers”, *Journal of Modern Optics*, no.  
5, vol. 51, pp. 627-632, 2004
- <sup>26</sup> C.H.Kua, Y.C.Lam, C.Yang, K.Youcef-Toumi “Bioparticle manipulation using  
Dielectrophoresis”

- <sup>27</sup> <http://www.bangslabs.com/products/bangs/guide.php>
- <sup>28</sup> Technote # 208 Bangs Laboratories Inc. "Microsphere Sizing".
- <sup>29</sup> <http://www3.interscience.wiley.com/cgi-bin/abstract/104032942/ABSTRACT>
- <sup>30</sup> TechNote # 206 Bangs Laboratories Inc. "Equations".
- <sup>31</sup> R.J Tonucci, B.L. Justus, A.J. Campillo, C.E. Ford. International conference on Quantum electronics, Science, vol. 258, pp. 783-785, 1992
- <sup>32</sup> A.J.Campillo Naval Research Laboratory "Science and Technology for New DoD Capabilities: Interdisciplinary Research examples in optical science at NRL"
- <sup>33</sup> Joseph Ladislav Wiza "Microchannel Plate Detectors", Reprinted from Nuclear Instruments and Methods, vol.162, pp. 587- 601, 1979
- <sup>34</sup> <http://www.metallographic.com>
- <sup>35</sup> <http://www.zhdanov.ru/classified-catalogue/b-companies/barnstead-thermolyne/hot-plates-stirrers1.pdf>
- <sup>36</sup> [http://www.2spi.com/catalog/misc\\_lab/shaker3.shtml](http://www.2spi.com/catalog/misc_lab/shaker3.shtml)
- <sup>37</sup> <http://www.instechlabs.com/Support/manuals/HA33Manual.pdf>
- <sup>38</sup> <http://www.microscopyu.com/>
- <sup>39</sup> <http://www.microscopyu.com/articles/optics/objectiveproperties.html>
- <sup>40</sup> [http://efunda.com/formulae/fluids/calc\\_pipe\\_friction.cfm](http://efunda.com/formulae/fluids/calc_pipe_friction.cfm)